Extended Data Table 2 | *cis*-eQTL of RA risk SNPs

a

RA risk SNP	Chr.	Position (bp)	eQTL gene	Cis-eQTL effect of best proxy SNP				Cis-eQTL effect of top eQTL SNP			
				Proxy SNP	Position (bp)	eQTL *P*	r^2	eQTL SNP	Position (bp)	eQTL *P*	r^2
chr1:2523811	1	2,523,811	*PLCH2*	rs10910099	2,533,552	2.2E-18	0.87	rs2494435	2,359,280	2.6E-45	<0.25
			TNFRSF14	rs2843401	2,528,133	1.1E-28	0.87	rs734999	2,513,216	2.1E-90	0.43
rs227163	1	7,961,206	*PARK7*	rs227163	7,961,206	4.6E-10	1.00	rs3766606	8,022,197	1.0E-53	<0.25
rs28411352	1	38,278,579	*MANEAL, YRDC*	rs2306627	38,260,503	3.9E-09	0.84	rs2306426	36,451,618	7.7E-10	<0.25
			INPP5B	rs2306627	38,260,503	7.5E-23	0.84	rs4072980	38,456,106	1.2E-113	<0.25
			SF3A3	rs2306627	38,260,503	3.3E-17	0.84	rs4072980	38,456,106	1.1E-190	<0.25
			FHL3	rs2306627	38,260,503	1.1E-11	0.84	rs4634868	38,465,315	9.8E-198	<0.25
rs2476601	1	114,377,568	*PTPN22*	rs2476601	114,377,568	3.4E-10	1.00	rs7555634	114,367,116	5.3E-43	<0.25
rs2228145	1	154,426,970	*AQP10*	rs6684439	154,395,839	3.3E-06	0.89	rs6668968	154,293,675	3.8E-40	<0.25
			IL6R	rs4129267	154,426,264	3.2E-27	1.00	rs4537545	154,418,879	2.0E-29	0.96
			UBE2Q1	rs4129267	154,426,264	9.7E-08	1.00	rs6660775	154,538,554	3.9E-21	<0.25
rs2317230	1	157,674,997	*FCRL5*	rs3761959	157,669,278	1.7E-09	0.87	rs6427386	157,530,097	9.8E-198	<0.25
			FCRL3	rs7528684	157,670,816	9.8E-198	0.87	rs2210913	157,668,993	9.8E-198	0.87
rs4656942	1	160,831,048	*LY9*	rs4656942	160,831,048	2.7E-96	1.00	rs576334	160,797,514	5.8E-195	<0.25
rs72717009	1	161,405,053	*SDHC*	rs12731669	161,410,458	5.5E-05	0.97	rs16832871	161,335,758	1.4E-142	<0.25
			FCGR2B	rs12731669	161,410,458	4.2E-83	0.97	rs6674499	161,618,151	9.8E-198	<0.25
rs17668708	1	198,640,488	*PTPRC*	rs17669032	198,653,174	5.2E-05	0.97	rs2296618	198,666,232	2.1E-05	0.78
rs1980422	2	204,610,396	*CD28*	rs1980421	204,610,004	7.3E-18	1.00	rs2140148	204,572,140	8.1E-21	0.47
rs10028001	4	79,502,972	*ANXA3*	rs10028001	79,502,972	1.1E-04	1.00	rs4975144	79,474,040	1.4E-09	<0.25
rs2561477	5	102,608,924	*PAM*	rs411648	102,602,902	2.2E-113	1.00	rs2431321	102,118,794	9.8E-198	<0.25
			GIN1	rs2288786	102,600,754	1.3E-06	1.00	rs42431	102,400,063	2.6E-13	0.43
rs657075	5	131,430,118	*ACSL6*	rs657075	131,430,118	3.8E-12	1.00	rs253946	131,330,461	9.2E-26	0.32
chr6:14103212	6	14,103,212	*CD83*	rs12530098	14,107,197	2.6E-24	1.00	rs16874672	14,087,484	2.2E-26	0.90
rs2234067	6	36,355,654	*KCTD20*	rs4713969	36,349,008	8.2E-05	0.99	rs4711453	36,439,391	3.1E-32	<0.25
			STK38	rs4713969	36,349,008	1.4E-06	0.99	rs1812018	36,557,976	6.8E-15	<0.25
			-	rs4713969	36,349,008	2.1E-26	0.99	rs10947614	36,573,822	1.1E-146	<0.25
			SFRS3	rs4713969	36,349,008	2.6E-11	0.99	rs7743396	36,579,252	1.5E-52	<0.25
rs9373594	6	149,834,574	*C6orf72*	rs9377224	149,853,707	4.0E-06	1.00	rs9322189	149,909,933	1.8E-15	0.30
			NUP43	rs9377224	149,853,707	4.1E-64	1.00	rs9688350	150,052,113	9.8E-198	0.27
rs2451258	6	159,506,600	*RSPH3*	rs2485363	159,506,121	5.0E-05	1.00	rs12216499	159,368,524	2.0E-119	<0.25
rs1571878	6	167,540,842	*RNASET2*	rs1571878	167,540,842	9.8E-198	1.00	rs429083	167,383,972	9.8E-198	0.39
chr7:128580042	7	128,580,042	*TNPO3*	rs3807306	128,580,680	1.4E-150	0.81	rs3807306	128,580,680	1.4E-150	0.81
			-	rs3807306	128,580,680	2.4E-32	0.81	rs10229001	128,599,397	4.5E-49	0.48
			IRF5	rs3807306	128,580,680	9.8E-198	0.81	rs7807018	128,640,188	9.8E-198	0.48
rs2736337	8	11,341,880	*C8orf13,C8orf12*	rs2736340	11,343,973	1.6E-174	0.99	rs4840568	11,351,019	3.8E-175	0.92
			BLK	rs1478901	11,347,833	1.8E-120	0.99	rs998683	11,353,000	1.5E-120	0.95
rs10985070	9	123,636,121	*TRAF1*	rs10985070	123,636,121	3.9E-72	1.00	rs2416804	123,676,396	3.8E-73	0.96
			PHF19	rs10985070	123,636,121	2.9E-10	1.00	rs10760129	123,700,183	2.2E-10	0.95
			C5	rs10985070	123,636,121	4.9E-68	1.00	rs2416811	123,789,634	2.0E-146	0.31
rs947474	10	6,390,450	-	rs947474	6,390,450	6.5E-06	1.00	rs12416248	6,391,031	1.1E-43	<0.25
rs2671692	10	50,097,819	*WDFY4*	rs2671692	50,097,819	3.0E-09	1.00	rs7072606	49,933,974	1.1E-50	<0.25
rs968567	11	61,595,564	*C11orf10*	rs968567	61,595,564	3.1E-39	1.00	rs174538	61,560,081	2.5E-67	0.40
			FADS1	rs968567	61,595,564	8.1E-62	1.00	rs968567	61,595,564	8.1E-62	1.00
			FADS2	rs968567	61,595,564	4.8E-34	1.00	rs968567	61,595,564	4.8E-34	1.00
rs10774624	12	111,833,788	*SH2B3*	rs653178	112,007,756	1.7E-19	0.86	rs2239195	111,881,309	1.0E-33	<0.25
			ALDH2	rs653178	112,007,756	8.7E-07	0.86	rs16941669	112,245,637	4.4E-50	<0.25
rs4780401	16	11,839,326	*TXNDC11*	rs11075010	11,826,013	8.3E-09	0.93	rs12919035	11,821,508	4.4E-12	0.49
rs72634030	17	5,272,580	*ZNF594*	rs8080217	5,164,761	8.7E-11	0.88	rs2071456	5,031,946	1.5E-12	0.65
			C17orf87	rs8080217	5,164,761	3.3E-05	0.88	rs2641232	5,087,602	1.4E-53	<0.25
			-	rs8080217	5,164,761	3.6E-70	0.88	rs7426	5,288,983	9.8E-198	<0.25
			NUP88	rs8080217	5,164,761	3.3E-27	0.88	rs1989946	5,313,152	8.9E-96	<0.25
			MIS12	rs8080217	5,164,761	8.5E-10	0.88	rs1805448	5,384,327	2.2E-35	<0.25
rs1877030	17	37,740,161	*FBXL20*	rs12937013	37,665,571	3.4E-15	1.00	rs8076462	37,400,025	3.1E-42	<0.25
			PPP1R1B	rs1877030	37,740,161	1.8E-10	1.00	rs879606	37,781,849	8.0E-18	0.41
			-	rs11657058	37,699,378	3.9E-05	1.00	rs7219814	37,478,801	2.1E-111	<0.25
			IKZF3	rs4795385	37,733,148	8.8E-24	1.00	rs2517955	37,843,681	5.2E-82	0.33
chr17:38031857	17	38,031,857	-	rs907092	37,922,259	6.6E-11	0.90	rs7219814	37,478,801	2.1E-111	<0.25
			IKZF3	rs11557467	38,028,634	3.3E-05	0.84	rs9896940	37,895,975	3.1E-25	<0.25
			GSDMB	rs10852936	38,031,714	9.8E-198	0.98	rs9901146	38,043,343	9.8E-198	0.84
			ORMDL3	rs10852936	38,031,714	9.8E-198	0.98	rs8076131	38,080,912	9.8E-198	0.86
rs2469434	18	67,544,046	*CD226*	rs1610555	67,543,147	2.3E-33	0.99	rs763361	67,531,642	2.4E-50	0.66
rs4239702	20	44,749,251	*CD40*	rs4239702	44,749,251	1.3E-34	1.00	rs745307	44,747,086	1.5E-72	<0.25
rs73194058	21	34,764,288	*IL10RB*	rs11702844	34,759,876	1.3E-11	0.97	rs1058867	34,669,381	3.0E-69	<0.25
			IFNAR1	rs11702844	34,759,876	8.0E-12	0.97	rs2257167	34,715,699	4.2E-73	<0.25
			TMEM50B	rs11702844	34,759,876	3.1E-11	0.97	rs1059293	34,809,693	2.2E-103	<0.25
			-	rs11702844	34,759,876	2.8E-34	0.97	rs2834217	34,822,150	9.8E-198	<0.25
rs1893592	21	43,855,067	*UBASH3A*	rs1893592	43,855,067	6.4E-92	1.00	rs1893592	43,855,067	6.4E-92	1.00
rs2236668	21	45,650,009	*ICOSLG*	rs7278940	45,648,992	3.7E-06	1.00	rs3788111	45,668,171	8.4E-16	<0.25
rs11089637	22	21,979,096	-	rs11089637	21,979,096	9.8E-198	1.00	rs5754217	21,939,675	9.8E-198	0.87
rs909685	22	39,747,671	*SYNGR1*	rs909685	39,747,671	1.0E-140	1.00	rs909685	39,747,671	1.0E-140	1.00
			MAP3K7IP1	rs909685	39,747,671	1.3E-05	1.00	rs5750824	39,830,123	5.9E-07	0.28

b

SNP	Chr.	Position (bp)	eQTL gene	Nominal *P* for cis-eQTL	
				$CD4^+$ T-cell	$CD14^+16^-$ Monocyte
rs28411352	1	38,278,579	*INPP5B*	0.022	**3.6E-16**
			FHL3	0.081	**8.9E-13**
rs2317230	1	157,674,997	*FCRL3*	**3.5E-06**	0.87
rs9653442	2	100,825,367	*AFF3*	**5.2E-08**	0.18
rs7731626	5	55,444,683	*IL6ST*	**2.3E-07**	0.0087
			ANKRD55	**4.1E-14**	0.43
rs2234067	6	36,355,654	*ETV7*	2.9E-04	**1.1E-10**
rs9373594	6	149,834,574	*NUP43*	5.4E-04	**1.5E-05**
rs1571878	6	167,540,842	*RNASET2*	**6.9E-20**	**1.3E-05**
rs67250450	7	28,174,986	*JAZF1*	**3.6E-17**	2.0E-04
chr7:128580042*	7	128,580,042	*TNPO3*	1.0E-04	**3.0E-07**
rs10985070	9	123,636,121	*MEGF9*	**3.3E-06**	0.10
			PSMD5	0.017	**1.8E-05**
			PHF19	0.0016	**5.6E-06**
rs968567	11	61,595,564	*FADS2*	**1.4E-31**	**8.9E-35**
			FADS1	**2.1E-32**	0.094
rs11605042	11	72,411,664	*STARD10*	0.82	**1.0E-07**
rs4409785	11	95,311,422	*SESN3*	**1.5E-11**	0.43
rs773125	12	56,394,954	*SUOX*	0.27	**1.1E-09**
rs1633360	12	58,108,052	*TSPAN31*	0.13	**1.0E-05**
			METTL21B	**1.4E-09**	**4.0E-10**
rs9603616	13	40,368,069	*COG6*	0.0011	**1.2E-05**
rs4780401	16	11,839,326	*TXNDC11*	**1.3E-05**	0.62
rs72634030	17	5,272,580	*MIS12*	0.0039	**1.3E-05**
rs1877030	17	37,740,161	*STARD3*	0.048	**4.5E-05**
chr17:38031857†	17	38,031,857	*GSDMA*	**2.1E-06**	0.63
			GSDMB	**4.3E-11**	0.19
			ORMDL3	**6.8E-09**	0.0098
rs4239702	20	44,749,251	*CD40*	0.31	**1.7E-08**
rs73194058	21	34,764,288	*IFNGR2*	0.096	**1.9E-06**
			TMEM50B	**7.5E-07**	0.013
rs1893592	21	43,855,067	*UBASH3A*	**3.8E-14**	0.92

a, *cis*-eQTL of PBMCs in the RA risk SNPs. Significant *cis*-eQTLs of RA risk SNPs is indicated (FDR $q < 0.05$). SNPs and positions are based on the positive strand of NCBI build 37. Linkage disequilibrium of the proxy SNPs evaluated in the eQTL study and the best *cis*-eQTL SNP in the region with the RA risk SNPs is indicated as r^2 values. When the expression probe was not assigned to any genes, the eQTL gene is labelled with a dash. **b**, *cis*-eQTL of T cells and monocytes in the RA risk SNPs. Significant *cis*-eQTLs of RA risk SNPs are indicated in bold (gene-based permutation $P < 0.05$).

* *cis*-eQTL of the proxy SNP (rs3807307, $r^2 = 0.96$) was evaluated.

† *cis*-eQTL of the proxy SNP (rs11557466, $r^2 = 0.98$) was evaluated.

Journal of Human Genetics (2013), 1–3

www.nature.com/jhg

SHORT COMMUNICATION

Significant association between *CYP3A5* polymorphism and blood concentration of tacrolimus in patients with connective tissue diseases

Kosuke Tanaka[1], Chikashi Terao[1], Koichiro Ohmura[2], Meiko Takahashi[1], Ran Nakashima[2], Yoshitaka Imura[2], Hajime Yoshifuji[2], Naoichiro Yukawa[2], Takashi Usui[2], Takao Fujii[2], Tsuneyo Mimori[2] and Fumihiko Matsuda[1]

Although the association between *CYP3A5* polymorphism and blood concentration of tacrolimus (TAC) in patients with solid organ transplantation was established, whether the association is also true in patients with connective tissue disease (CTD) who usually receive small amount of TAC is uncertain. Here, we performed a quantitative linear regression analysis to address the association between *CYP3A5* and blood TAC concentration in patients with CTD. A total of 72 patients with CTD were recruited in the current study and genotyped for rs776746 in *CYP3A5*, which showed strong association with TAC concentration in patients with solid organ transplantation. The blood trough concentration of TAC after taking 3 mg per day was retrospectively obtained for each patient. As a result, allele A of rs776746 showed a significant association with a decreasing blood concentration of TAC ($P = 0.0038$). Those who are carrying at least one copy of the A allele displayed decreased mean concentration of TAC by 31.0% compared with subjects with GG genotype. Rs776746 is associated with concentrations of TAC in patients with CTD.
Journal of Human Genetics advance online publication, 19 December 2013; doi:10.1038/jhg.2013.129

Keywords: connective tissue disease; pharmacogenetics; tacrolimus

Tacrolimus (FK506, TAC) is a calcineurin inhibitor isolated from *Streptomyces tsukubaensis*[1] and one of the many types of powerful immunosuppressants that are frequently used for solid organ transplantation to prevent organ rejection.[2] TAC is also used for patients with connective tissue disease (CTD) including rheumatoid arthritis (RA), systemic lupus erythematosus, polymyositis and dermatomyositis to control disease activity.[3,4] TAC is metabolized mainly by cytochrome P450 (CYP) 3A in the liver and intestine.[5] Because TAC concentration is highly variable among patients, to predict TAC concentration to achieve therapeutic effect is a big challenge. Previous studies revealed that the variation of TAC concentration is largely attributable to different expressions of *CYP3A* in patients of organ transplantation. Patients carrying *CYP3A5*3* determined by the G allele of rs776746 were shown to have high TAC concentration than patients with the A allele.[5,6] Although TAC is a substrate for P-glycoprotein encoded by the *ABCB1* gene, effects of polymorphisms in *ABCB1* on TAC concentration are inconclusive.[6–8] Genetic studies have been performed mainly recruiting patients with organ transplantation to date. The number of previous studies focusing on TAC concentration in non-organ transplantation subjects is limited.[9,10]

When TAC is given to patients with CTD, the dosage is around 3 mg per day,[3,4] which is much lower than that given to patients of organ transplantation. For example, patients with renal transplantation receive 0.3 mg kg^{-1} per day at the transplantation and 0.12 mg kg^{-1} per day as maintainance.[11] In addition, although recipients of renal transplantation take TAC twice daily,[11] patients with only CTD take a single dose of TAC per day. The effect of *CYP3A5* on TAC concentrations with low TAC exposure in patients with CTD has not been studied so far. Furthermore, chronic, systemic and autoimmune inflammatory process in CTD may influence the metabolism and concentration of TAC. Thus, whether the association between polymorphisms of *CYP3A5* and TAC concentrations can be observed in patients with CTD remained unclear. Here, we performed an association study to address this point.

This study was designed in accordance with the Helsinki Declaration and approved by the ethics committee of Kyoto University Graduate School and Faculty of Medicine. A total of 72 subjects with CTD who were prescribed to take a single dose of 3 mg of TAC every day in the evening at the Department of Rheumatology and Clinical Immunology, Kyoto University Graduate School of Medicine from December 2005 to December 2012 were enrolled in this study. Written informed consent was obtained from all the participants. Patients

[1]Center for Genomic Medicine, Kyoto University Graduate School of Medicine, Kyoto, Japan and [2]Department of Rheumatology and Clinical Immunology, Kyoto University Graduate School of Medicine, Kyoto, Japan
Correspondence: Dr C Terao, Center for Genomic Medicine, Kyoto University Graduate School of Medicine, Kyoto 606-8507, Japan.
E-mail: a0001101@kuhp.kyoto-u.ac.jp
Received 26 September 2013; revised 25 November 2013; accepted 25 November 2013

took PROGRAF (Astellas Pharma Inc., Tokyo, Japan) capsules containing 1 or 0.5 mg TAC. CTD patients fulfilled criteria for each disease, namely, American College of Rheumatology (ACR) criteria for RA in 1987[12] or ACR/EULAR criteria in 2010,[13] for systemic lupus erythematosus,[14] polymyositis and dermatomyositis[15] and for polyarteritis nodosa and microscopic polyangiitis.[16] Information of age, sex, weight, serum creatinine and date of prescription, dosage, and blood concentration of TAC were obtained from clinical charts retrospectively by the system previously described.[17] Information of prescription and dosage of corticosteroid was also obtained. TAC concentration data were obtained at least one week after prescription was initiated or changed. The data of concurrent use of cyclosporine or bosentan, contraindication due to interaction with TAC, was excluded. Estimated glomelular filtration ratio (eGFR) was inferred by serum creatinine, age and sex. The blood trough TAC concentration with 3 mg TAC (around 12 h after taking TAC) was used. TAC concentrations were quantified by two measurements according to measuring time; namely, microparticle enzyme immunoassay (MEIA, IMxTM-TACRO II, Abbott Laboratories, Green Oaks, IL, USA) until May 2009 and chemiluminescent immunoassay (CLIA, ARCHITECT_TACRO, Abbott Laboratories) from May 2009. These measurements can quantify even low TAC concentrations ($\sim$1.5 and $\sim$0.5 ng ml^{-1}, respectively). When TAC concentrations were available for both measurements in a patient, data of CLIA with lower measuring limit of TAC concentrations was used. A total of 63 and 9 patients were quantified by CLIA and MEIA, respectively (hereafter termed as CLIA group and MEIA group, respectively). When multiple TAC concentrations were available, the mean of them was adopted. Calculations were performed on the basis of logarithm of TAC concentrations to obtain normal distribution and to avoid excess influence of extreme data.

The summary of the subjects in the current study is shown in Table 1. Log-transformation of TAC concentration supported applying linear regression analysis. When we analyzed correlations between TAC concentration and age, sex, weight, eGFR, dosage or usage of corticosteroid or the presence of RA or systemic lupus erythematosus by single linear regression analysis, none of them displayed overall significant associations ($P \geqslant 0.083$). However, because presence of RA showed a suggestive association in MEIA group ($P = 0.0091$), we used presence of RA as a covariate. Rs776746, whose G allele determined *CYP3A5*3*, was selected on the basis of previous studies and genotyped by the Taqman assay (Applied Biosystems Inc, Foster city, CA, USA). As a result, no deviation from Hardy–Weinberg equilibrium was observed ($P = 0.13$). Although previous reports comparing different measurement methods of blood concentration of TAC showed good correlations ($r \geqslant 0.84$) and did not detect discrepancy even in ranges of low concentrations,[18,19] MEIA was suggested to underestimate TAC concentrations in low levels.[19] Thus we analyzed the associations in CLIA and MEIA groups separately, and the overall associations were estimated by meta-analysis using inverse-variance method. We found a significant decreasing effect of the A allele of rs776746 on TAC concentration ($P = 0.0038$, Figure 1). Both MEIA and CLIA groups showed the comparable effect sizes, supporting the accuracy of the result (Table 2). Patients who carried A allele had 31.0% lower mean concentration than those who were homozygote for G allele. Although the current and the previous studies[11] showed a good fit of the dose-dependent model of rs776746, there are also conflicting reports.[6,20] Considering the limited number of subjects with AA genotype, the dose-dependent effect of rs776746 should be regarded as inconclusive. Meta-analysis of the recessive model resulted in a comparable result ($P = 0.0035$, AA + GA vs GG).

The current study provided evidence that TAC concentration was strongly influenced by *CYP3A5* in patients with CTD even taking a small amount of TAC. Our results showed the same direction of A allele of rs776746 and comparable effect sizes in the previous studies using patients of solid organ transplantation.[5,6] Disease-specific influence on TAC concentrations was not clear. As this study contained relatively small number of subjects and low TAC concentrations around the measurement limits might be associated with diminished accuracy, these results should be replicated by a larger number of patients with CTD, also including other populations. Because the predictive model of TAC concentration is proposed in

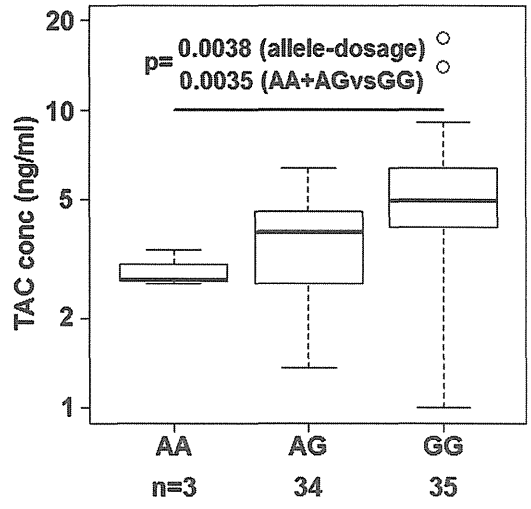

Figure 1 Association between TAC concentration and the polymorphism in *CYP3A5* in patients with CTD. The obtained or inferred TAC concentrations adjusted for 3mg TAC are shown according to rs776746 genotypes. *Y* axis is shown in log scale. The mean concentrations are 2.88, 3.57 and 5.10 ng ml^{-1} for AA, AG and GG genotypes, respectively. TAC concentrations were adjusted for MEIA group.

Table 1 Summary of subjects in the current study

	Study subjects
Age[a]	48.94 ± 17.24
Sex	Male 13, female 59
Disease	RA: 22, SLE: 43, DM: 3, PM: 2, PAN: 1, mPA: 1

Abbreviations: DM, dermatomyositis; mPA, microscopic polyangiitis; PAN, polyarteritis nodosa; PM, polymyositis; RA, rheumatoid arthritis; SLE, systemic lupus.erythematosus.
[a]mean ± s.d.

Table 2 Association between rs776746 and TAC concentration in multiple regression analysis

	Number	*Beta*	*s.e.*	P-*value*
CLIA	63	0.106	0.041	0.012
MEIA	9	0.161	0.12	0.22
Overall	72	0.112	0.039	0.0038

Abbreviations: CLIA, chemiluminescent immunoassay; MEIA, microparticle enzyme immunoassay; TAC, tacrolimus.
Statistics adjusted by rheumatoid arthritis presence.

patients of organ transplantation, it will be interesting to construct a predictive model of TAC concentration in patients with CTD.

CONFLICT OF INTEREST

The authors declare no conflict of interest.

ACKNOWLEDGEMENTS

We would like to thank all the patients registered in this study. This study was supported by Kyoto University Step-up grant.

1 Kino, T., Hatanaka, H., Miyata, S., Inamura, N., Nishiyama, M., Yajima, T. *et al.* FK-506, a novel immunosuppressant isolated from a Streptomyces. II. Immunosuppressive effect of FK-506 in vitro. *J. Antibiot. (Tokyo)* **40,** 1256–1265 (1987).
2 Scott, L. J., McKeage, K., Keam, S. J. & Plosker, G. L. Tacrolimus: a further update of its use in the management of organ transplantation. *Drugs* **63,** 1247–1297 (2003).
3 Takeuchi, T., Kawai, S., Yamamoto, K., Harigai, M., Ishida, K. & Miyasaka, N. Post-marketing surveillance of the safety and effectiveness of tacrolimus in 3,267 Japanese patients with rheumatoid arthritis. *Mod. Rheumatol.* **24,** 8–16 (2014).
4 Takahashi, S., Hiromura, K., Sakurai, N., Matsumoto, T., Ikeuchi, H., Maeshima, A. *et al.* Efficacy and safety of tacrolimus for induction therapy in patients with active lupus nephritis. *Mod. Rheumatol.* **21,** 282–289 (2011).
5 Hesselink, D. A., van Gelder, T. & van Schaik, R. H. The pharmacogenetics of calcineurin inhibitors: one step closer toward individualized immunosuppression? *Pharmacogenomics* **6,** 323–337 (2005).
6 Tsuchiya, N., Satoh, S., Tada, H., Li, Z., Ohyama, C., Sato, K. *et al.* Influence of CYP3A5 and MDR1 (ABCB1) polymorphisms on the pharmacokinetics of tacrolimus in renal transplant recipients. *Transplantation* **78,** 1182–1187 (2004).
7 Tada, H., Tsuchiya, N., Satoh, S., Kagaya, H., Li, Z., Sato, K. *et al.* Impact of CYP3A5 and MDR1(ABCB1) C3435T polymorphisms on the pharmacokinetics of tacrolimus in renal transplant recipients. *Transplant. Proc.* **37,** 1730–1732 (2005).
8 Vafadari, R., Bouamar, R., Hesselink, D. A., Kraaijeveld, R., van Schaik, R. H., Weimar, W. *et al.* Genetic polymorphisms in ABCB1 influence the pharmacodynamics of tacrolimus. *Ther. Drug. Monit.* **35,** 459–465 (2013).
9 Hirai, F., Takatsu, N., Yano, Y., Satou, Y., Takahashi, H., Ishikawa, S. *et al.* CYP3A5 genetic polymorphisms affect the pharmacokinetics and short-term remission in patients with ulcerative colitis treated with tacrolimus. *J. Gastroenterol. Hepatol.* (in press).
10 Shi, X. J., Geng, F., Jiao, Z., Cui, X. Y., Qiu, X. Y. & Zhong, M. K. Association of ABCB1, CYP3A4*18B and CYP3A5*3 genotypes with the pharmacokinetics of tacrolimus in healthy Chinese subjects: a population pharmacokinetic analysis. *J. Clin. Pharm. Ther.* **36,** 614–624 (2011).
11 Niioka, T., Kagaya, H., Miura, M., Numakura, K., Saito, M., Inoue, T. *et al.* Pharmaceutical and genetic determinants for interindividual differences of tacrolimus bioavailability in renal transplant recipients. *Eur. J. Clin. Pharmacol.* **69,** 1659–1665 (2013).
12 Arnett, F. C., Edworthy, S. M., Bloch, D. A., McShane, D. J., Fries, J. F., Cooper, N. S. *et al.* The American Rheumatism Association 1987 revised criteria for the classification of rheumatoid arthritis. *Arthritis. Rheum.* **31,** 315–324 (1988).
13 Aletaha, D., Neogi, T., Silman, A. J., Funovits, J., Felson, D. T., Bingham, C. O. 3rd *et al.* Rheumatoid arthritis classification criteria: an American College of Rheumatology/European League Against Rheumatism collaborative initiative. *Arthritis. Rheum.* **62,** 2569–2581 (2010).
14 Hochberg, M. C. Updating the American College of Rheumatology revised criteria for the classification of systemic lupus erythematosus. *Arthritis. Rheum.* **40,** 1725 (1997).
15 Bohan, A. & Peter, J. B. Polymyositis and dermatomyositis (first of two parts). *N. Engl. J. Med.* **292,** 344–347 (1975).
16 Bloch, D. A., Michel, B. A., Hunder, G. G., McShane, D. J., Arend, W. P., Calabrese, L. H. *et al.* The American College of Rheumatology 1990 criteria for the classification of vasculitis. Patients and methods. *Arthritis. Rheum.* **33,** 1068–1073 (1990).
17 Terao, C., Hashimoto, M., Yamamoto, K., Murakami, K., Ohmura, K., Nakashima, R. *et al.* Three groups in the 28 joints for rheumatoid arthritis synovitis–Analysis using more than 17,000 assessments in the KURAMA database. *PLoS One* **8,** e59341 (2013).
18 Ju, M. K., Chang, H. K., Kim, H. J., Huh, K. H., Ahn, H. J., Kim, M. S. *et al.* Is the affinity column-mediated immunoassay method suitable as an alternative to the microparticle enzyme immunoassay method as a blood tacrolimus assay? *Transplant. Proc.* **40,** 3673–3678 (2008).
19 Marubashi, S., Nagano, H., Kobayashi, S., Eguchi, H., Takeda, Y., Tanemura, M. *et al.* Evaluation of a new immunoassay for therapeutic drug monitoring of tacrolimus in adult liver transplant recipients. *J. Clin. Pharmacol.* **50,** 705–709 (2010).
20 Hesselink, D. A., van Schaik, R. H., van der Heiden, I. P., van der Werf, M., Gregoor, P. J., Lindemans, J. *et al.* Genetic polymorphisms of the CYP3A4, CYP3A5, and MDR-1 genes and pharmacokinetics of the calcineurin inhibitors cyclosporine and tacrolimus. *Clin. Pharmacol. Ther.* **74,** 245–254 (2003).

The Journal of Rheumatology

The Journal of Rheumatology Volume 41, no. 2

A Clinical, Pathological, and Genetic Characterization of Methotrexate-associated Lymphoproliferative Disorders

Noriyuki Yamakawa, Masakazu Fujimoto, Daisuke Kawabata, Chikashi Terao, Momoko Nishikori, Ran Nakashima, Yoshitaka Imura, Naoichiro Yukawa, Hajime Yoshifuji, Koichiro Ohmura, Takao Fujii, Toshiyuki Kitano, Tadakazu Kondo, Kimiko Yurugi, Yasuo Miura, Taira Maekawa, Hiroh Saji, Akifumi Takaori-Kondo, Fumihiko Matsuda, Hironori Haga and Tsuneyo Mimori

J Rheumatol 2014;41;293-299
http://www.jrheum.org/content/41/2/293

A Clinical, Pathological, and Genetic Characterization of Methotrexate-associated Lymphoproliferative Disorders

Noriyuki Yamakawa, Masakazu Fujimoto, Daisuke Kawabata, Chikashi Terao, Momoko Nishikori, Ran Nakashima, Yoshitaka Imura, Naoichiro Yukawa, Hajime Yoshifuji, Koichiro Ohmura, Takao Fujii, Toshiyuki Kitano, Tadakazu Kondo, Kimiko Yurugi, Yasuo Miura, Taira Maekawa, Hiroh Saji, Akifumi Takaori-Kondo, Fumihiko Matsuda, Hironori Haga, and Tsuneyo Mimori

ABSTRACT. ***Objective.*** Methotrexate-associated lymphoproliferative disorders (MTX-LPD) often regress spontaneously during MTX withdrawal, but the prognostic factors remain unclear. The aim of our study was to clarify the clinical, histological, and genetic factors that predict outcomes in patients with MTX-LPD.

Methods. Patients with MTX-LPD diagnosed between 2000 and 2012 were analyzed retrospectively regarding their clinical course, site of biopsy, histological typing, Epstein-Barr virus (EBV) *in situ* hybridization and immunostaining, and HLA type.

Results. Twenty-one patients, including 20 with rheumatoid arthritis (RA) and 1 with polymyositis, were analyzed. The mean dose of MTX was 6.1 mg/week and the mean duration of treatment was 71.1 months. Clinically, 5 patients were diagnosed with EBV-positive mucocutaneous ulcer (EBVMCU) and had polymorphic histological findings. The proportion of those patients successfully treated solely by withdrawal of MTX was significantly greater than that of those without EBVMCU (75% vs 7.7%, p = 0.015). The HLA-B15:11 haplotype was more frequent in patients with EBV+ RA with MTX-LPD than in healthy Japanese controls (p = 0.0079, Bonferroni's method). EBV latency classification and HLA typing were not associated with the prognosis of MTX-LPD in our cohort.

Conclusion. Our data demonstrate that patients in the EBVMCU, a specific clinical subgroup of MTX-LPD, had a better clinical outcome when MTX was withdrawn than did other patients with MTX-LPD. (First Release Dec 15 2013; J Rheumatol 2014;41:293–9; doi:10.3899/jrheum.130270)

Key Indexing Terms:
RHEUMATIC DISEASES | RHEUMATOID ARTHRITIS
SKIN MANIFESTATIONS | HLA ANTIGENS | HEMATOPOIETIC SYSTEM

Methotrexate (MTX)-associated lymphoproliferative disorders (LPD) are a lymphoid proliferation or lymphoma that occur in patients immunosuppressed with MTX, classified as a part of the "other iatrogenic immunodeficiency-associated lymphoproliferative disorders" category by the World Health Organization (WHO) in 2008[1]. Because MTX has recently gained acceptance as a first-line therapy for rheumatoid arthritis (RA)[2,3] and other systemic

From the Department of Rheumatology and Clinical Immunology, the Department of Diagnostic Pathology, the Center for Genomic Medicine, and the Department of Hematology and Oncology, Kyoto University Graduate School of Medicine; the Department of Transfusion Medicine and Cell Therapy, Kyoto University Hospital; the HLA Foundation Laboratory, Kyoto, Japan.

N. Yamakawa, MD, Department of Rheumatology and Clinical Immunology; M. Fujimoto, MD, the Department of Diagnostic Pathology; D. Kawabata, MD, PhD, Department of Rheumatology and Clinical Immunology; C. Terao, MD, PhD, Department of Rheumatology and Clinical Immunology, and the Center for Genomic Medicine; M. Nishikori, MD, PhD, Department of Hematology and Oncology; R. Nakashima, MD, PhD; Y. Imura, MD, PhD; N. Yukawa, MD, PhD; H. Yoshifuji, MD, PhD; K. Ohmura, MD, PhD; T. Fujii, MD, PhD, Department of Rheumatology and Clinical Immunology; T. Kitano, MD; T. Kondo, MD, PhD, Department of Hematology and Oncology, Kyoto University Graduate School of Medicine; K. Yurugi; Y. Miura, MD, PhD; T. Maekawa, MD, PhD, Department of Transfusion Medicine and Cell Therapy, Kyoto University Hospital; H. Saji, BSc, HLA Foundation Laboratory; A. Takaori-Kondo, MD, PhD, Department of Hematology and Oncology; F. Matsuda, MD, PhD, Center for Genomic Medicine; H. Haga, MD, PhD, Department of Diagnostic Pathology; T. Mimori, MD, PhD, Department of Rheumatology and Clinical Immunology, Kyoto University Graduate School of Medicine.

Address correspondence to Dr. D. Kawabata, Kyoto University, Department of Rheumatology and Clinical Immunology, Shogoin-Kawahara-cho, 54 Sakyo-ku, Kyoto 606-8507, Japan. E-mail: yakugo@gmail.com

Accepted for publication October 8, 2013.

rheumatic diseases (SRD), the incidence of MTX-LPD is expected to increase. A better understanding of this important disease is somewhat limited by its rarity. Epstein-Barr virus (EBV) infection is thought to play an important role in the pathogenesis of MTX-LPD, although EBV can only be detected on histopathologic examination in about half the cases of MTX-LPD[4].

Under normal circumstances, EBV-specific cytotoxic T lymphocytes (EBV-CTL) act to suppress EBV-infected B cells. However, if the function of EBV-CTL is impaired by immunosuppressants, such as MTX or by aging, EBV-infected B cells are reactivated to induce B cell proliferation, leading to the development of LPD. There is speculation that MTX could reactivate latent EBV infection, because patients with SRD treated with regimens that include MTX have higher mean EBV loads in their blood than those who do not[5]. EBV-related LPD (EBV-LPD) can be categorized into 3 types on the basis of their expression of EBV-encoded small RNA (EBER), EBV latent membrane protein-1 (LMP1), and EBV nuclear antigen-2 (EBNA2): latency I (EBER+, LMP-1–, EBNA2–) as seen in Burkitt's lymphoma; latency II (EBER+, LMP-1+, EBNA-2–) as seen in Hodgkin's lymphoma or nasopharyngeal carcinoma; and latency III (EBER+, LMP-1+, EBNA-2+) as seen in posttransplant LPD (PT-LPD)[6]. EBV-LPD frequently occurs in immunosuppressed patients and its prognosis appears to vary widely.

LPD with EBV-positive mucocutaneous ulcer (EBVMCU) has been reported as a distinct disease entity with a self-limiting and indolent clinical course[7]. EBVMCU is found in various conditions of immunosuppression, including MTX-LPD or in age-related immunosenescence. The latter is characterized by age-related EBV+ B cell LPD (Age-LPD) on a background of EBV infection in elderly patients without immunodeficiency[8]. Although MTX-LPD often shows spontaneous regression, it is not clear whether MTX-LPD with EBVMCU has a better prognosis. The aim of our study was to clarify the clinical, histological, and genetic factors predictive of a good prognosis in patients with MTX-LPD.

MATERIALS AND METHODS

Patients. Twenty-one patients with SRD who developed MTX-LPD between 2000 and 2012 were included in our study. There were 20 with RA and 1 with polymyositis (PM). Of the 20 patients with RA, 3 had RA overlapping with Sjögren syndrome (SS), 1 had RA with systemic lupus erythematosus (SLE), and 1 had RA with polymyalgia rheumatica (PMR). The diagnoses of RA, PM, SS, SLE, and PMR were made according to the American College of Rheumatology classification criteria. The stage of RA was evaluated by Steinbrocker's classification and the stage of LPD by Ann Arbor classification. After the histologic diagnosis of MTX-LPD was made, MTX was withdrawn in all patients. Necessity of chemotherapy was determined according to the histology, karyotypes, stages, or clinical judgment of poor response to MTX withdrawal.

Ethics statement. The study was conducted in compliance with the Declaration of Helsinki and was approved by the Kyoto University Ethics Committee Review Board; written informed consent was obtained from all patients.

Histological analysis. Two pathologists performed histological analysis of specimens from each patient. Diagnoses were made in accordance with the criteria specified in *WHO Tumors of Hematopoietic and Lymphoid Tissues,* fourth edition[1]. Immunostaining of paraffin sections was performed using monoclonal antibodies against LMP1 (Clone CS.1-4, Dako) and EBNA2 (M7004, PE2, Dako). The presence of EBER was determined by *in situ* hybridization (ISH) using a peptide nucleic acid (PNA) ISH detection kit (K5201, Dako) and an EBER PNA Probe/Fluorescein kit (Y5200, Dako).

Typing of HLA. HLA-A, B, and DR typing studies of 16 cases of RA with MTX-LPD and 96 control cases of RA without MTX-LPD diagnosed in our department were undertaken using the PCR-Luminex method. The frequency of each HLA allele was analyzed with reference to the Japanese HLA laboratory database (http://hla.or.jp/haplo/haplonavi.php?type=haplo&lang=ja), which includes over 20,000 cases.

Statistical analysis. Data are expressed as mean ± SD. Comparisons of HLA and histological data were made using Fisher's exact test. Each allele seen in more than 2 cases was assessed with significant level corrected p value (Pc) by Bonferroni's method. A Kaplan-Meier plot of the chemotherapy-free survival was evaluated by the log-rank test. All analyses were performed using PASW Statistics 18 (18.0.0) and statistical significance was defined as $p < 0.05$.

RESULTS

Clinical and pathological details of patients with MTX-LPD. The clinical, pathological, and genetic characteristics of 21 cases of MTX-LPD are shown in Table 1; 17 (81%) were female; the mean age was 65.8 ± 7.5 years (range 52 to 79 yrs). The average dose of MTX was 6.1 ± 1.7 mg/week; treatment duration was 71.1 ± 57.8 months. Staging of RA was undertaken using Steinbrocker's classification; 1 patient fulfilled the criteria for stage I, 3 for stage II, 3 for stage III, and 13 for stage IV. Three patients (cases 1, 5, and 15) were treated with infliximab. Seventeen out of 20 RA cases (85%) were rheumatoid factor (RF)-positive and 7 out of 14 cases (50%) were anticitrullinated protein antibody (ACPA)-positive.

The pathological findings were as follows: 10 cases were diagnosed with diffuse large B cell lymphoma (DLBCL), 7 with polymorphic lymphoproliferative disorder (p-LPD), 3 with HL, and 1 with small B cell lymphoma that later transformed into DLBCL. The biopsy site was extranodal in 12 cases (57%); all 7 cases of p-LPD were extranodal, while 3 cases of HL were nodal. Of the 10 cases of DLBCL, half were extranodal and half nodal. Twelve out of 20 cases (60%) were EBER-positive, while 8 cases of 19 (42%) were LMP1-positive and 3 cases out of 19 (16%) were EBNA2-positive. EBV latency was classified by means of EBER, LMP1, and EBNA2 expression into 4 groups: EBV-negative and latencies I–III. Representative histological images are shown in Figure 1. The cases diagnosed as p-LPD comprised 7 of the 12 patients in latency I–III groups; but there were none among the 8 patients in the EBV-negative group ($p = 0.012$). Extranodal involvement was found in 8 of 12 patients in the latency I–III groups but only 3 of 8 in the EBV-negative group. EBVMCU was diagnosed in 5 cases (cases 1, 2, 4, 5, and 21), each charac-

Table 1. Clinical and pathological findings in 21 cases of methotrexate-associated lymphoproliferative disorders (MTX-LPD).

No.	Age	Sex	Disease	Dose of MTX, mg/week	Duration of MTX, mos	E/N	Site of Biopsy	Histology	EBER	LMP1	EBNA2	EBV Latency	LPD Stage	IPI	Therapy and Response	Response (final state)	Prognosis	Followup period, mos
1	76	F	RA	8.0	27	E(MCU)	left eyelid	p-LPD	(+)	(+)	(+)	III	I	L	W → CR	CR	A	24
2	64	F	RA	8.0	120	E(MCU)	buccal mucosa	p-LPD	(+)	(+)	(+)	III	IV	HI	W	ND	D#1	1
3	71	F	RA	8.0	184	E	left latero-abdominal nodule	p-LPD	(+)	(+)	(+)	III	IV	H	R-CHOP → PR → oral VP-16 → CR	CR	A	31
4	59	F	RA	5.0	63	E(MCU)	left eyelid	p-PLD	(+)	(+)	(–)	II	I	H	W→ CR	CR	A	37
5	61	F	RA	10.0	74	E(MCU)	right lower leg ulcer	p-PLD	(+)	(+)	(–)	II	IV	H	R-CHOP → CR	CR	A	25
6	65	F	RA SS	4.0	27	N	left axillary lymph node	HL	(+)	(+)	(–)	II	II	LI	W → CR → relapse → ABVD, C-MOPP → PR → RT → CR	CR	A	79
7	65	F	RA	5.0	66	N	right axillary lymph node	HL	(+)	(+)	(–)	II	IV	HI	W → CR → relapse → ABVD → CR	CR	D#2	17
8	58	F	RA	4.0	66	N	inguinal lymph node	SBL	(+)	(+)	(–)	II	II	L	CHOP, RT → CR → relapse → observe → R-ICE, CHASER, auto-PBSCT (MEAM) → CR	CR	D#3	92
9	67	F	RA SS	6.0	16	E	parotid gland	DLBCL	(+)	(–)	(–)	I	III	H	R-CHOP → CR → relapse → R-DeVIC → PR → RT, CHASER, R-ESHAP, mini-MEAM, GEM, CPT-11 → PD	PD	D	90
10	61	F	RA	6.0	193	N	right cervical lymph node	DLBCL	(+)	(–)	(–)	I	III	LI	R-CHOP → CR	CR	A	45
11	79	M	RA	8.0	169	E	right forearm	p-LPD	(+)	(–)	(–)	I	I	LI	W → CR	CR	A	9
12	66	M	RA	6.0	46	N	left submandibular lymph node	DLBCL	(–)	(–)	(–)	n	IV	HI	R → CR → relapse → CHOP → PD	PD	D	27
13	72	F	RA SLE	6.0	ND	N	right submandibular lymph node	DLBCL	(–)	(–)	(–)	n	II	LI	R-CHOP → CR → relapse → R-DeVIC	PD	A	48
14	74	F	RA	7.0	74	N	right cervical lymph node	DLBCL	(–)	(–)	(–)	n	II	LI	W → CR	CR	A	32
15	52	F	RA SS	5.0	47	E	precordial skin	DLBCL	(–)	(–)	(–)	n	IV	HI	R-CHOP → CR	CR	A	84
16	76	M	RA	4.0	ND	N	right axillary lymph node	HL	(–)	(–)	(–)	n	III	HI	W	ND	A	1
17	71	M	RA PMR	5.0	7	N	right cervical lymph node	DLBCL	(–)	(–)	(–)	n	II	HI	R-CHOP → PR	PR	A	8
18	62	F	RA	8.0	21	E	right orbital fossa	DLBCL	(–)	(–)	(–)	n	II	LI	R-CHOP → CR	CR	A	15
19	56	F	RA	5.5	98	E	left submandibular skin	DLBCL	(–)	(–)	(–)	n	II	L	W → CR	CR	A	14
20	71	F	RA	6.0	48	E	lumbar mass	DLBCL	NE	NE	NE	ND	II	LI	R-CHOP, RT → CR	CR	A	132
21	56	F	PM	4.0	4	E(MCU)	left lower leg ulcer	p-LPD	(+)	NE	NE	ND	I	L	W → CR	CR	A	33

No. 1: Died soon from intercurrent disease (myelitis and sepsis). No. 2: Died from bleomycin-induced interstitial pneumonia. No. 3: died from pneumocystis pneumonia. PM: polymyositis; RA: rheumatoid arthritis; SS: Sjögren syndrome; SLE: systemic lupus erythematosus, PMR: polymyalgia rheumatica; E: extranodal; MCU: mucocutaneous ulcer lesion; N: nodal; EBV: Epstein-Barr virus; DLBCL: diffuse large B cell lymphoma; EBER: EBV-encoded small RNA; p-LPD: polymorphic lymphoproliferative disorder; SBL: small B cell lymphoma; HL: Hodgkin lymphoma; n: EBV-negative; NE: not examined; ND: not determined; IPI: international prognostic index; L: low risk; LI: low-intermediate risk; HI: high-intermediate risk; H: high risk; W: withdrawal of MTX only; R-CHOP: rituximab, cyclophosphamide, hydroxydaunorubicin, vincristine and prednisolone; ABVD: adriamycin, bleomycin, vinblastine and dacarbazine; C-MOPP: cyclophosphamide, vincristine, prednisolone and procarbazine; RT: radiotherapy; R-ICE: rituximab, ifosfamide, carboplatin and etoposide; MEAM: ranimustine (MCNU), etoposide, cytarabine and melphalan; R-DeVIC: rituximab, dexamethasone, etoposide, ifosfamide and carboplatin; R-ESHAP: rituximab, etoposide, prednisolone, high-dose cytarabine and cisplatin; GEM: gemcitabine; CPT-11: irinotecan; CR: complete remission; PD: progressive disease; PR: partial remission; A: alive; D: dead; auto-PBSCT: autologous peripheral blood stem cell transplantation; CHASER: cyclophosphamide, cytarabine, dexamethasone, etoposide, and rituximab

terized by sharply demarcated skin ulcers with an erythematous appearance accompanied by crusting and necrosis (Figure 2) which, on histological examination, were found to be polymorphic with a mixture of lymphocytes and immunoblasts. Lymphocytic vasculitis was seen in 3 out of 5 cases (cases 2, 5, and 21). Four out of 5 cases (80%) of EBVMCU were seropositive.

HLA typing of patients with MTX-LPD. As shown in Table 2, we found that 3 cases out of 16 were heterozygous for the HLA-B15:11 allele. The allele frequency of HLA-B15:11

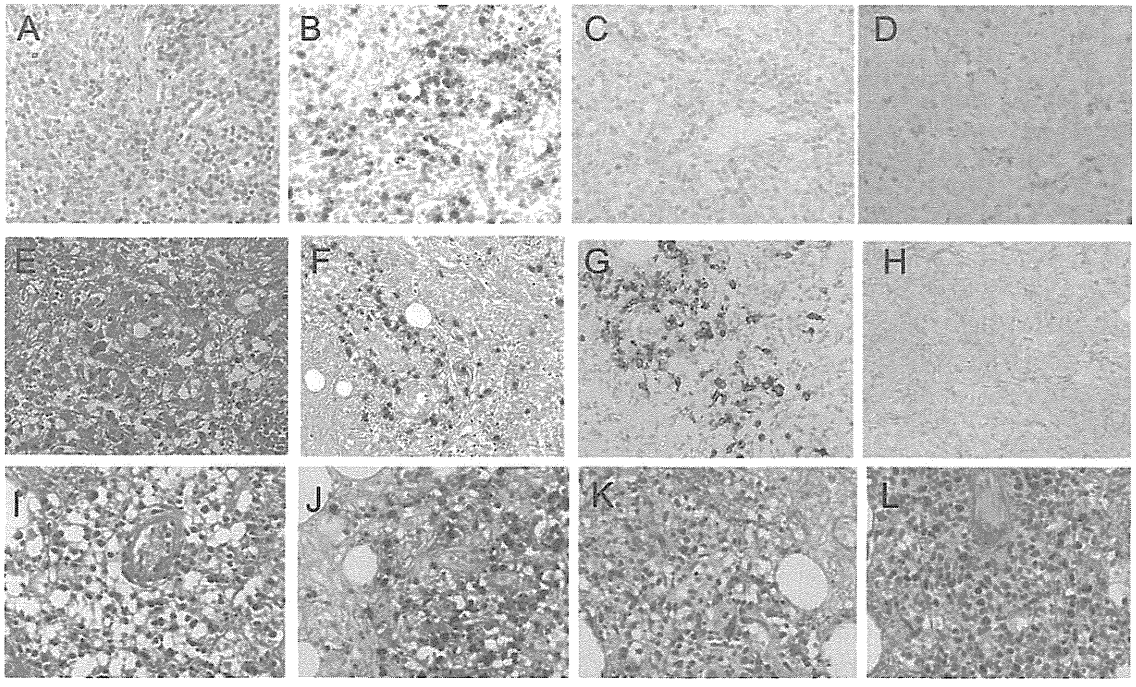

Figure 1. Pathological findings in 3 cases of MTX-LPD classified by EBV latency. A-D. DLBCL (case 10, latency I). E-H. Polymorphic LPD (case 4, latency II). I-L. Polymorphic LPD (case 3, latency III). Pathological findings are shown by H&E (A, E, I), EBER (B: positive, F: positive, J: positive), LMP1 (C: negative, G: positive, K: positive), and EBNA2 (D: negative, H: negative, L: positive) staining. MTX-LPD: methotrexate-associated lymphoproliferative disorders; EBV: Epstein-Barr virus; DLBCL: diffuse large B cell lymphoma; EBER: EBV-encoded small RNA; LMP1: EBV latent membrane protein-1; EBNA2: EBV nuclear antigen-2.

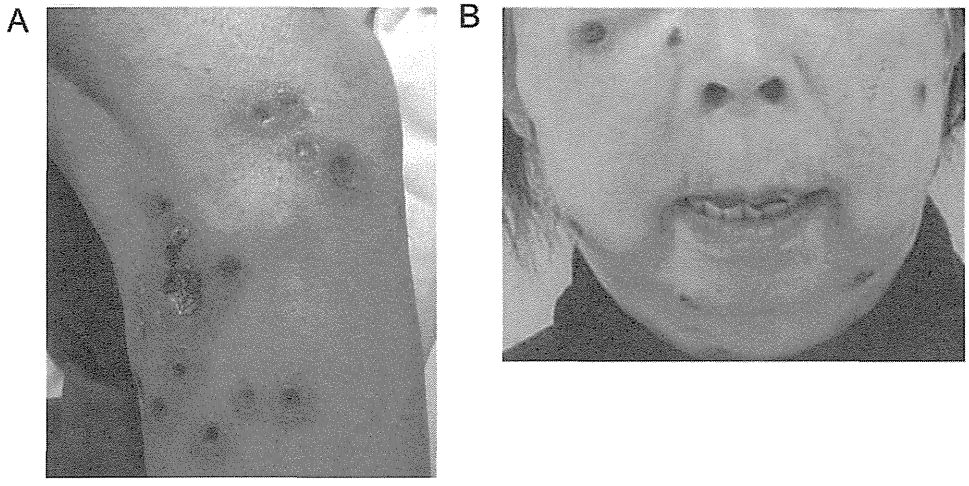

Figure 2. Two representative cases with skin manifestations of EBV-positive mucocutaneous ulcer (EBVMCU). Typical skin manifestations of EBVMCU (A: case 5, B: case 2) are shown. Characteristic sharply demarcated skin ulcers with an erythematous appearance accompanied by crusting and necrosis can be seen.

was higher in EBV+ RA with MTX-LPD, compared with the control JHD group and that of the Japanese RA cohort (Pc = 0.0079 and 0.024, respectively, Table 3). RA-shared epitopes were observed in 11 of 16 cases (69%), a significantly higher proportion than in healthy Japanese controls (38%, n = 1508; p = 0.018), but not in Japanese patients with RA (n = 759)[9].

Clinical course of patients with MTX-LPD. MTX was withdrawn in all cases at the time of LPD diagnosis. When examining the need for chemotherapy within 18 months of

Table 2. HLA-A, B, and DR alleles of 16 cases of RA with MTX-LPD.

No.	HLA-A	HLA-B	HLA-DR
1	11:01/24:02	35:01/48:01	04:05*/09:01
3	02:01/24:02	15:11/40:02	09:01/14:02*
4	24:02/26:01	15:07/40:02	04:03/09:01
5	24:02	07:02/52:01	01:01*/15:02
6	02:06/26:01	15:11/39:01	04:10*/14:06*
7	02:01/26:01	35:01/55:02	04:05*/04:06
9	24:02	07:02/54:01	04:05*/08:02
10	11:01	48:01/54:01	04:05*/15:01
11	02:01/02:07	15:11/46:01	09:01
12	24:02/26:01	40:02/52:01	04:05*/09:01
13	02:01/24:02	40:01/52:01	04:05*/15:02
14	24:02/33:03	44:03/52:01	08:03/15:02
15	24:02	52:01	15:02
18	02:01	07:02/15:01	01:01*/15:01
19	02:01/02:06	48:01/54:01	04:05*/04:07
20	24:02	51:01/59:01	01:01*/04:05*

* Rheumatoid arthritis shared epitope. RA: rheumatoid arthritis; MTX-LPD: methotrexate-associated lymphoproliferative disorders.

diagnosis, withdrawal of MTX alone was more successful for those in the EBVMCU group (n = 4, cases 1, 4, 5, and 21) than the other cases (n = 13; 75% vs 7.7%, p = 0.015; Figure 3). Because the observation periods were at most 2 years in the majority of cases, we were unable to calculate longterm prognosis. Five patients (cases 2, 7, 8, 9, and 12) died; LPD recurred in 2 patients at 90 months (case 9) and 21 months (case 12) from the original diagnosis and did not respond to continued chemotherapy. One patient (case 2) died from intercurrent myelitis and sepsis soon after the diagnosis of LPD and 1 patient (case 7) died from bleomycin-induced pneumonia.

One patient (case 8) was first diagnosed with EBV-positive small B cell lymphoma (SBL). Although chemotherapy resulted in partial remission, she had an indolent clinical course without chemotherapy until the tumor progressed and histopathological study revealed EBV-negative DLBCL with the same phenotype as the SBL. A clonal relationship between the 2 lymphomas was not proven; however, Richter syndrome was suspected clinically. With regard to the predicted unfavorable prognosis, she was treated with autologous peripheral blood stem cell transplantation, but she died of pneumocystis pneumonia under continuous immunosuppression. Although 2 cases of EBVMCU (cases 2 and 5) were included in Ann Arbor stage IV, each had a favorable clinical outcome.

DISCUSSION

We have shown that the presence of EBVMCU appears to confer a better prognosis in patients with MTX-LPD. Most of our patients with positive outcomes had been diagnosed with EBVMCU. Of the 12 cases of MTX-LPD with mucocutaneous ulcer reported in the literature[7,10,11,12,13,14,15,16,17] all except 1[17] were EBV-positive and all 9 cases with available data showed complete remission without chemotherapy.

EBVMCU was first reported to be a favorable prognostic indicator in a case series of 26 patients (consisting of 19 with Age-LPD and 7 with iatrogenic immunodeficiency-associated LPD including 4 with MTX-LPD)[7], but the incidence of EBVMCU in MTX-LPD was not known. Our study shows that the incidence of EBVMCU in EBV+ MTX-LPD is 42% (5 out of 12), which is higher than that of EBVMCU in Age-LPD (13%, 16 cases out of 122)[18].

Age-LPD is believed to be a consequence of an underlying immunological deficit, or immunosenescence of the T cell receptor (TCR) repertoire[19,20] — a natural degeneration of the immune system that occurs with aging. Considering the high average age of our cases, age-related immunosenescence might be partly involved in the development of MTX-LPD. This may be revealed by decreases in the TCR repertoire in the future.

Only a few cases of EBV latency in MTX-LPD have been reported; those of EBV latency among MTX-LPD, PT-LPD, and Age-LPD are summarized in Table 4[21,22,23]. Other case series include 53 cases of LPD in a variety of autoimmune diseases, including 4 cases of MTX-LPD, in which all 16 cases of EBV+ LPD were in latency II[24]. Taken together, these data suggest that EBV+ MTX-LPD is more

Table 3. Risk allele of RA with MTX-LPD in Japanese population.

	Total Allele Nos.	(+)	(–)	Frequency of Allele in Control Cases	p*	Pc Value**	OR	95% CI
HLA-B15:11								
in RA with MTX-LPD, n = 16	32	3	29	0.0096[1]	0.0036	0.061	10.0	3.0–32.8
				0.0052[2]	0.0097	0.16	18.5	1.9–183.4
in RA with MTX-LPD without EBVMCU, n = 13	26	3	23	0.0096[1]	0.0020	0.032	13.4	4.0–45.0
				0.0052[2]	0.0056	0.090	24.9	2.5–249.5
in EBV+ RA with MTX-LPD, n = 9	18	3	15	0.0096[1]	0.00066	0.0079	18.2	5.3–62.3
				0.0052[2]	0.0020	0.024	38.2	3.7–390.0

[1] Japanese healthy control. [2] RA control. * 2 × 2 Fisher's exact study. ** Corrected with Bonferroni's method. RA: rheumatoid arthritis; MTX-LPD: methotrexate-associated lymphoproliferative disorders; EBV: Epstein-Barr virus; EBVMCU: EBV-positive mucocutaneous ulcer.

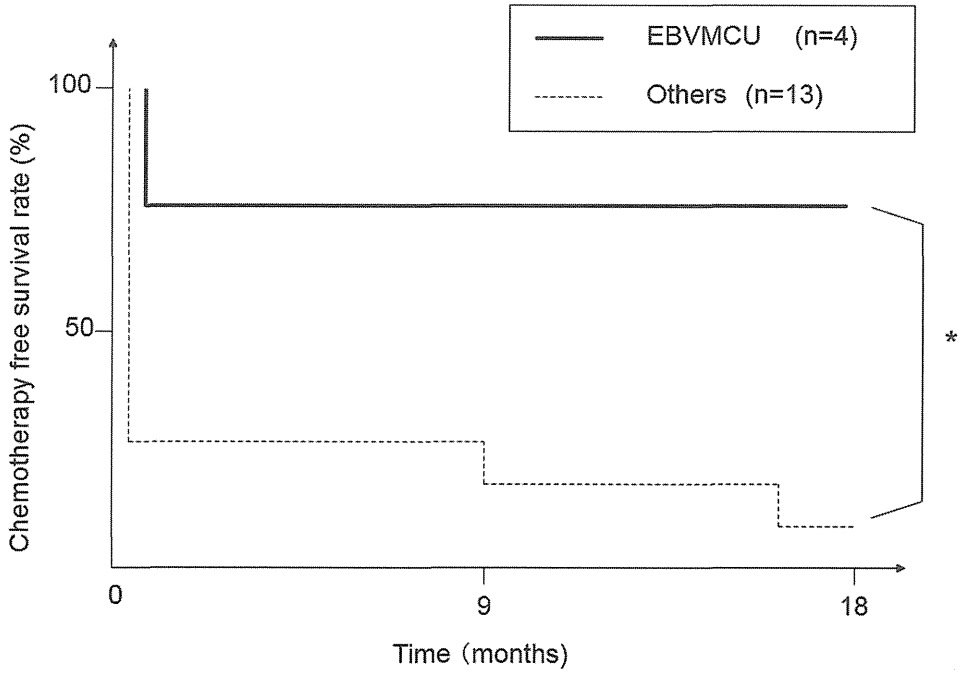

Figure 3. Chemotherapy-free survival. Kaplan-Meier curve shows chemotherapy-free survival within 18 months, comparing patients in the EBV-positive mucocutaneous ulcer (EBVMCU) group with those with other forms of MTX-LPD. Methotrexate was withdrawn in all cases. *Log-rank test, $p < 0.05$. MTX-LPD: methotrexate-associated lymphoproliferative disorders; EBV: Epstein-Barr virus.

Table 4. EBV latency classification among MTX-LPD, PT-LPD, and Age-LPD.

Disease	Year	Author	Cases	I	II	III
PT-LPD	2003	Birkeland	16	1	8	7
Age-LPD	2009	Asano	26	0	19	7
MTX-LPD	2007	Miyazaki	3	0	1	2
MTX-LPD	2013	present case series	11	3	5	3

MTX-LPD: methotrexate-associated lymphoproliferative disorders; PT-LPD: posttransplant lymphoproliferative disorders.

likely to be in latency II, followed by latency III. This observation also appears to hold true for PT-LPD and Age-LPD. PT-LPD has been generally categorized as latency III[25], but is often seen to be in latency II. Cases of Age-LPD were also found to be mainly in latency II. Nonetheless, the latency classification had no value in predicting the prognosis of MTX-LPD in our cohort. The utility of EBV latency in MTX-LPD remains unknown.

Although the pathogenesis of EBVMCU is unclear, lymphocytic vasculitis was observed in more than half our cases of EBVMCU. In EBV-positive LPD, the Mig monokine, induced by interferon-γ (IFN-γ), and IFN-γ inducible protein-10 (mainly produced by reactive cells including endothelial cells) are thought to be powerful instigators of vascular and tissue injuries[26]. Thus, we hypothesize that tissue necrosis and the impairment of local blood flow to the area of vascular damage might be pivotal to the pathogenesis of EBVMCU. Although it is unclear why patients with MTX-LPD who developed EBVMCU had a better prognosis, several factors might be responsible. One possibility is that the mucocutaneous ulcer is so conspicuous that patients seek medical help more promptly, when diagnosis is relatively straightforward and the disease is in an earlier, potentially reversible stage. Thus, the prompt cessation of MTX may lead to a good outcome.

Our study is the first, to our knowledge, to have conducted HLA typing, revealing that HLA-B15:11 could be a risk allele in EBV+ RA with MTX-LPD. Notably, all 3 HLA-B15:11-positive cases were EBV-positive and 2 were polymorphic, indicating that this allele may be linked to the susceptibility to EBV infection and development of LPD. In our study, HLA-B15:11 had no correlation with HLA-shared epitopes, RF, or ACPA. To the best of our knowledge, there have been no reports of any relationship between this allele and other diseases. The identification of a genetic risk factor could help to clarify the pathogenesis of

LPD and to achieve safer therapy for patients who might be at risk of LPD if their RA is treated with MTX. Because this is a retrospective study, there are some limitations, and a larger scale prospective trial is needed to clarify the pathogenesis of this disease.

We have demonstrated that cases of EBVMCU, a subgroup of MTX-LPD, were all histologically polymorphic and had a more favorable outcome by withdrawing MTX alone. In addition, we found that the frequency of the HLA-B15:11 allele was significantly increased in our cohort, which suggests that it may be a risk factor for EBV+ RA with MTX-LPD.

ACKNOWLEDGMENT

The authors thank Dr. Toda (Kyoto University, Center for Anatomical Studies) for performing immunostaining studies and Dr. Inoko (Tokai University, Department of Molecular Science) for kindly providing the HLA reference data of Japanese patients with rheumatoid arthritis.

REFERENCES

1. Gaulard P. Swerdlow SH, Harris NL, Jaffe ES, Sundstrom C. Other iatrogenic immunodeficiency-associated lymphoproliferative disorders. In: Swerdlow SH, Campo E, Harris NL, Jaffe ES, Pileri SA, Stein H, et al, eds. Tumours of haematopoietic and lymphoid tissues. Pathology & genetics. World Health Organization classification of tumours. 4th ed. Lyon: IARC Press; 2008:350-1.
2. Weinblatt ME, Coblyn JS, Fox DA, Fraser PA, Holdsworth DE, Glass DN, et al. Efficacy of low-dose methotrexate in rheumatoid arthritis. N Engl J Med 1985;312:818-22.
3. Rath T, Rubbert A. Drug combinations with methotrexate to treat rheumatoid arthritis. Clin Exp Rheumatol 2010;5 Suppl 61:S52-7.
4. Harris NL, Swerdlow SH. Methotrexate-associated lymphoproliferative disorders. In: Jaffe ES, Harris NL, Stein H, Vardiman JW, eds. Tumours of haematopoietic and lymphoid tissues. Pathology & genetics. World Health Organization classification of tumours. 3rd ed. Lyon: IARC Press; 2001:270-1.
5. Feng WH, Cohen JI, Fischer S, Li L, Sneller M, Goldbach-Mansky R, et al. Reactivation of latent Epstein-Barr virus by methotrexate: a potential contributor to methotrexate-associated lymphomas. J Natl Cancer Inst 2004;96:1691-702.
6. Young LS, Rickinson AB. Epstein-Barr virus: 40 years on. Nat Rev Cancer 2004;4:757-68.
7. Dojcinov SD, Venkataraman G, Raffeld M, Pittaluga S, Jaffe ES. EBV positive mucocutaneous ulcer—a study of 26 cases associated with various sources of immunosuppression. Am J Surg Pathol 2010;34:405-17.
8. Oyama T, Ichimura K, Suzuki R, Suzumiya J, Ohshima K, Yatabe Y, et al. Senile EBV+ B-cell lymphoproliferative disorders: a clinicopathologic study of 22 patients. Am J Surg Pathol 2003;27:16-26.
9. Ohmura K, Terao C, Maruya E, Katayama M, Matoba K, Shimada K, et al. Anti-citrullinated peptide antibody-negative RA is a genetically distinct subset: a definitive study using only bone-erosive ACPA-negative rheumatoid arthritis. Rheumatology 2010;49:2298-304.
10. Hashizume H, Uchiyama I, Kawamura T, Suda T, Takigawa M, Tokura Y. Epstein-Barr virus-positive mucocutaneous ulcers as a manifestation of methotrexate-associated B-cell lymphoproliferative disorders. Acta Derm Venereol 2012;92:276-7.
11. Curry JL, Prieto VG, Jones DM, Vega F, Duvic M, Diwan AH. Transient iatrogenic immunodeficiency-related B-cell lymphoproliferative disorder of the skin in a patient with mycosis fungoides/Sezary syndrome. J Cutan Pathol 2011;38:295-7.
12. Shimura C, Satoh T, Takayama K, Yokozeki H. Methotrexate-related lymphoproliferative disorder with extensive vascular involvement in a patient with rheumatoid arthritis. J Am Acad Dermatol 2009;61:126-9.
13. Pastor-Nieto MA, Kilmurray LG, Lopez-Chumillas A, O'Valle F, Garcia-Del Moral R, Puig AM, et al. Methotrexate-associated lymphoproliferative disorder presenting as oral ulcers in a patient with rheumatoid arthritis [in Spanish]. Actas Dermosifiliogr 2009;100:142-6.
14. Uneda S, Sonoki T, Nakamura Y, Matsuoka H, Nakakuma H. Rapid vanishing of tumors by withdrawal of methotrexate in Epstein-Barr virus-related B cell lymphoproliferative disorder. Intern Med 2008;47:1445-6.
15. Tanaka A, Shigematsu H, Kojima M, Sakashita H, Kusama K. Methotrexate-associated lymphoproliferative disorder arising in a patient with adult Still's disease. J Oral Maxillofac Surg 2008;66:1492-5.
16. Maruani A, Wierzbicka E, Machet MC, Abdallah-Lotf M, de Muret A, Machet L. Reversal of multifocal cutaneous lymphoproliferative disease associated with Epstein-Barr virus after withdrawal of methotrexate therapy for rheumatoid arthritis. J Am Acad Dermatol 2007;5 Suppl:S69-71.
17. Clarke LE, Junkins-Hopkins J, Seykora JT, Adler DJ, Elenitsas R. Methotrexate-associated lymphoproliferative disorder in a patient with rheumatoid arthritis presenting in the skin. J Am Acad Dermatol 2007;56:686-90.
18. Dojcinov SD, Venkataraman G, Pittaluga S, Wlodarska I, Schrager JA, Raffeld M, et al. Age-related EBV-associated lymphoproliferative disorders in the Western population: a spectrum of reactive lymphoid hyperplasia and lymphoma. Blood 2011;117:4726-35.
19. Oyama T, Yamamoto K, Asano N, Oshiro A, Suzuki R, Kagami Y, et al. Age-related EBV-associated B-cell lymphoproliferative disorders constitute a distinct clinicopathologic group: a study of 96 patients. Clin Cancer Res 2007;13:5124-32.
20. Shimoyama Y, Yamamoto K, Asano N, Oyama T, Kinoshita T, Nakamura S. Age-related Epstein-Barr virus-associated B-cell lymphoproliferative disorders: special references to lymphomas surrounding this newly recognized clinicopathologic disease. Cancer Sci 2008;99:1085-91.
21. Miyazaki T, Fujimaki K, Shirasugi Y, Yoshiba F, Ohsaka M, Miyazaki K, et al. Remission of lymphoma after withdrawal of methotrexate in rheumatoid arthritis: relationship with type of latent Epstein-Barr virus infection. Am J Hematol 2007;82:1106-9.
22. Birkeland SA, Hamilton-Dutoit S. Is posttransplant lymphoproliferative disorder (PTLD) caused by any specific immunosuppressive drug or by the transplantation per se? Transplantation 2003;76:984-8.
23. Asano N, Yamamoto K, Tamaru J, Oyama T, Ishida F, Ohshima K, et al. Age-related Epstein-Barr virus (EBV)-associated B-cell lymphoproliferative disorders: comparison with EBV-positive classic Hodgkin lymphoma in elderly patients. Blood 2009;113:2629-36.
24. Hoshida Y, Tomita Y, Zhiming D, Yamauchi A, Nakatsuka S, Kurasono Y, et al. Lymphoproliferative disorders in autoimmune diseases in Japan: analysis of clinicopathological features and Epstein-Barr virus infection. Int J Cancer 2004;108:443-9.
25. Masucci MG. Epstein-Barr virus oncogenesis and the ubiquitin-proteasome system. Oncogene 2004;23:2107-15.
26. Teruya-Feldstein J, Jaffe ES, Burd PR, Kanegane H, Kingma DW, Wilson WH, et al. The role of Mig, the monokine induced by interferon-gamma, and IP-10, the interferon-gamma-inducible protein-10, in tissue necrosis and vascular damage associated with Epstein-Barr virus-positive lymphoproliferative disease. Blood 1997;90:4099-105.

DOI:10.1093/jnci/djt338
Advance Access publication December 7, 2013

BRIEF COMMUNICATION

Novel Germline Mutation in the Transmembrane Domain of *HER2* in Familial Lung Adenocarcinomas

Hiromasa Yamamoto, Koichiro Higasa, Masakiyo Sakaguchi, Kazuhiko Shien, Junichi Soh, Koichi Ichimura, Masashi Furukawa, Shinsuke Hashida, Kazunori Tsukuda, Nagio Takigawa, Keitaro Matsuo, Katsuyuki Kiura, Shinichiro Miyoshi, Fumihiko Matsuda, Shinichi Toyooka

Manuscript received July 7, 2013; revised October 14, 2013; accepted October 16, 2013.

Correspondence to: Shinichi Toyooka, MD, PhD, Okayama University Graduate School of Medicine, Dentistry and Pharmaceutical Sciences, Clinical Genomic Medicine/Thoracic, Breast and Endocrinological Surgery, 2-5-1 Shikata-cho, Kita-ku, Okayama, Okayama 700–8558, Japan (e-mail: toyooka@md.okayama-u.ac.jp).

We encountered a family of Japanese descent in which multiple members developed lung cancer. Using whole-exome sequencing, we identified a novel germline mutation in the transmembrane domain of the human epidermal growth factor receptor 2 (*HER2*) gene (G660D). A novel somatic mutation (V659E) was also detected in the transmembrane domain of *HER2* in one of 253 sporadic lung adenocarcinomas. Because the transmembrane domain of *HER2* is considered to be responsible for the dimerization and subsequent activation of the *HER* family and downstream signaling pathways, we performed functional analyses of these *HER2* mutants. Mutant HER2 G660D and V659E proteins were more stable than wild-type protein. Both the G660D and V659E mutants activated Akt. In addition, they activated p38, which is thought to promote cell proliferation in lung adenocarcinoma. Our findings strongly suggest that mutations in the transmembrane domain of *HER2* may be oncogenic, causing hereditary and sporadic lung adenocarcinomas.

JNCI J Natl Cancer Inst (2014) 106(1): djt338

Familial lung cancers are rare among human malignancies. Recent studies have reported that germline mutations in the epidermal growth factor receptor (*EGFR*) gene predispose the development of lung cancer. Reported familial lung adenocarcinomas with a germline *EGFR* mutation, such as T790M, carry secondary somatic *EGFR* mutations, including exon 19 deletion and exon 21 L858R mutation (1–4). We encountered a family of Japanese descent in which multiple members developed lung cancer (Figure 1). The proband (III-4) was a 53-year-old woman with multiple lung adenocarcinomas in bilateral lungs. She was a light smoker with a 1.2-pack-year history of smoking. She had undergone a left lower lobectomy for multiple lung adenocarcinomas at the age of 44 years. Her mother (II-4), a never smoker, also had multiple lung adenocarcinomas. Partial pulmonary resections of two tumors were performed for II-4 for the purpose of diagnosis after pleural dissemination was found during surgery, and multiple lesions were removed in a lobectomy or partial resections in III-4. A histological examination of the resected tumors in II-4 revealed nonmucinous adenocarcinoma in situ and nonmucinous minimally invasive adenocarcinoma, whereas

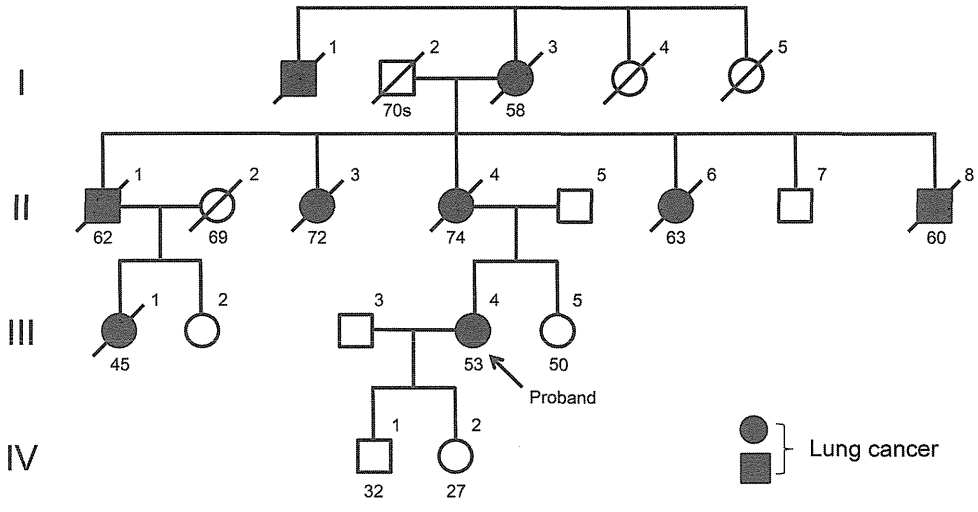

Figure 1. Pedigree chart of a Japanese family in which multiple members developed lung cancer. The **boxes** and **circles** indicate men and women, respectively. The **numbers** at the bottom of each member indicate the age at the time of death or the time of the analysis. An **oblique line** shows deceased family members. The proband (III-4) had multiple lung adenocarcinomas (**arrow**). Tumor tissue, nonmalignant lung tissue, and peripheral blood samples were obtained from III-4. The proband's mother (II-4) also had multiple lung adenocarcinomas, and tumor and nonmalignant lung tissue samples were available. The proband's father (II-5) and sister (III-5) were both unaffected, and peripheral blood samples were obtained from these individuals. Some family members who were not considered as critical for this study were excluded from the pedigree chart to preserve confidentiality. Whole-exome sequencing was performed for individuals II-4, II-5, III-4, and III-5.

the histological findings of pleural dissemination indicated mucus-containing adenocarcinoma. Those of III-4 contained various subtypes of adenocarcinoma, including nonmucinous and mucinous adenocarcinoma in situ and invasive mucinous adenocarcinoma. In addition, normal-appearing lung parenchyma obtained from a lobectomy in III-4 revealed innumerable small preinvasive lesions, implying the presence of precancerous changes throughout the lung (Supplementary Figure 1, available online). Sequencing analyses of *EGFR* exons 18 to 21 and *KRAS* as well as an immunohistochemical staining for ALK protein in the resected tumors indicated no genetic alterations in these genes. The pedigree chart suggested that lung cancer was inherited in an autosomal dominant manner.

After obtaining permission from the Institutional Review Board at Okayama University Hospital and informed consent from the patients and other family members, we performed a whole-exome sequencing study. Tumor DNA samples from II-4, tumor and peripheral blood DNA samples from III-4, and peripheral blood DNA samples from two unaffected family members (II-5 and III-5) were used for the analysis. The candidate germline alterations were restricted to 29 variants by comparing the whole-exome sequencing results between the patients and the unaffected family members. Among them, we focused on a point mutation in the human epidermal growth factor receptor 2 (*HER2/neu*) gene (NM_004448, G660D, GGC to GAC), which was located in exon 17 encoding the transmembrane domain of *HER2* (Supplementary Tables 1–3). This alteration was confirmed by direct sequencing (Figure 2A). We also confirmed that there was no copy number gain of *HER2* in the examined tumors based on the degree of read-depth in the whole-exome sequencing results. Of note, no mutations in genes known to cause lung cancers were detected for tumors from III-4 and II-4.

We considered that somatic mutations in the *HER2* transmembrane domain might act as driver mutations in lung cancer. Hence, we sequenced exon 17 of the *HER2*

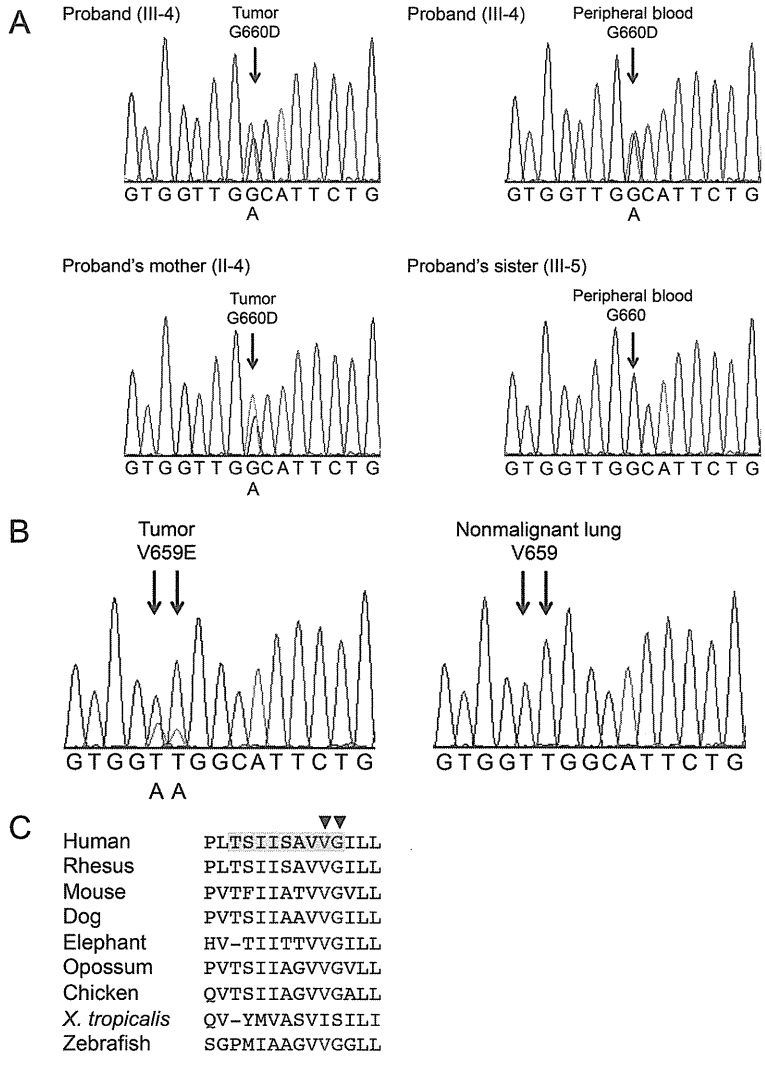

Figure 2. DNA and amino acid sequences in the transmembrane domain of *HER2*. **A**) Direct Sanger sequencing of the proband (III-4), her affected mother (II-4), and her unaffected sister (III-5). The results indicated that G660D was a germline mutation. **B**) Direct sequencing of a sporadic lung adenocarcinoma with a *HER2* V659E mutation. V659E was found to be of somatic origin based on the sequencing results of the peritumoral lung tissue from the same specimen. All the sequence variants were confirmed by independent polymerase chain reaction amplifications and were sequenced in both directions. **C**) Interspecies conservation of the transmembrane domain of *HER2* (UCSC Genome Browser, http://genome.ucsc.edu, accessed September 12, 2013). The **yellow highlight** indicates the N-terminal glycine zipper motif Thr^{652}-X_3-Ser^{656}-X_3-Gly^{660}, a tandem variant of a GG4-like motif of human *HER2*. Codons 659 and 660 in human *HER2* are highly conserved among the listed vertebrate species (shown in **red**). *X. tropicalis* = *Xenopus tropicalis*.

in the tumor samples of 315 sporadic non–small cell lung cancer patients, of which 253 were adenocarcinomas. Although the *HER2* G660D mutation was not detected, a novel nonsynonymous mutation, V659E (GTT to GAA), next to codon 660 was identified in one of these patients. This patient was histologically diagnosed as nonmucinous adenocarcinoma in situ, and the patient had neither smoking history nor apparent family history of lung cancer. This V659E mutation was certainly a somatic mutation because it was not identified in the peritumoral lung tissue of the same patient (Figure 2B). The alignment of *HER2* amino acid sequences showed high conservation of valine 659 and glycine 660 among vertebrates (Figure 2C).

HER2 somatic mutations have been reported in 2% to 4% of lung adenocarcinomas (5–7). However, all reported mutations were restricted to its tyrosine kinase domain (6,7). According to the cBioPortal for Cancer Genomics (http://www.cbioportal.org/public-portal/, accessed September 12, 2013), the same genetic mutation in the *HER2* has not been reported in any type of cancer. Interestingly, a previous study reported that a mutation in the transmembrane domain (V664E) of the rat *neu* gene, which corresponds to V659E in its human homolog *HER2*, induced oncogenic transformation (8). In addition, in vivo experiments showed that the *HER2* V659E mutation contributed to the stability of HER2 dimers, resulting in the dysregulated receptor activation and subsequent cell transformation (9,10). Furthermore, the novel mutations were located within the glycine zipper motif Thr^{652}-X_3-Ser^{656}-X_3-Gly^{660}, a tandem variant of the GG4-like motif, at the N-terminal portion of the transmembrane domain, which was critically related to the dimerization of HER2 (Figure 2C) (9,11). Accordingly, we performed a functional analysis of the mutant HER2 proteins. We found that the degradation of HER2 protein after the administration of cycloheximide was slower in G660D and V659E mutants as compared with wild-type (Supplementary Figure 2A), indicating the higher stability of the mutant proteins than wild-type protein. In addition, results of a phospho-mitogen–activated protein kinase array indicated the activation of Akt and p38α (data not shown). Indeed, Akt is known to be activated by HER2 by phosphatidylinositol 3-kinase and leads to increased cell growth and survival (12,13). Also, the activation of p38 was shown to contribute to the viability of lung adenocarcinoma cells derived from never or light smokers (14,15). A western blot analysis for Akt and p38 successfully confirmed the upregulation of both phospho-Akt and phospho-p38 expression in the mutant *HER2* transfectants (Supplementary Figure 2B).

Because the G660D alteration in *HER2* might have been the cause of the lung cancer in the pedigree studied, we investigated whether familial aggregation of cancer in other organs could be seen in this pedigree. We found that II-1 and II-6 developed renal and gastric cancers, respectively; however, both of them also had lung cancer. The reason why other types of clinically apparent malignances were rarely found in this pedigree is unclear. The G660D germline mutation may be tolerated in organs other than the lung.

This study had some limitations. First, the carcinogenic potential of the *HER2* mutation at the transmembrane domain should be confirmed in other models such as transgenic mice. Second, the rarity of these mutations in sporadic lung cancers may be the limitation for generalizability to other cases even if targeting therapies for similar types of *HER2* mutation were developed.

In conclusion, we identified a novel germline mutation in the transmembrane domain of the *HER2* in familial lung adenocarcinomas. Somatic mutation in the *HER2* transmembrane domain may be a possible cause of sporadic lung adenocarcinomas.

References

1. Bell DW, Gore I, Okimoto RA, et al. Inherited susceptibility to lung cancer may be associated with the T790M drug resistance mutation in EGFR. *Nat Genet*. 2005;37(12):1315–1316.
2. Ikeda K, Nomori H, Mori T, Sasaki J, Kobayashi T. Novel germline mutation: EGFR V843I in patient with multiple lung adenocarcinomas and family members with lung cancer. *Ann Thorac Surg*. 2008;85(4):1430–1432.
3. Ohtsuka K, Ohnishi H, Kurai D, et al. Familial lung adenocarcinoma caused by the EGFR V843I germ-line mutation. *J Clin Oncol*. 2011;29(8):e191–e192.
4. van Noesel J, van der Ven WH, van Os TA, et al. Activating germline R776H mutation in the epidermal growth factor receptor associated with lung cancer with squamous differentiation. *J Clin Oncol*. 2013;31(10):e161–e164.
5. Pao W, Girard N. New driver mutations in non-small-cell lung cancer. *Lancet Oncol*. 2011;12(2):175–180.
6. Shigematsu H, Takahashi T, Nomura M, et al. Somatic mutations of the HER2 kinase domain in lung adenocarcinomas. *Cancer Res*. 2005;65(5):1642–1646.
7. Stephens P, Hunter C, Bignell G, et al. Lung cancer: intragenic ERBB2 kinase mutations in tumours. *Nature*. 2004;431(7008):525–526.
8. Bargmann CI, Hung MC, Weinberg RA. Multiple independent activations of the neu oncogene by a point mutation altering the transmembrane domain of p185. *Cell*. 1986;45(5):649–657.
9. Bocharov EV, Mineev KS, Volynsky PE, et al. Spatial structure of the dimeric transmembrane domain of the growth factor receptor ErbB2 presumably corresponding to the receptor active state. *J Biol Chem*. 2008;283(11):6950–6956.
10. Fleishman SJ, Schlessinger J, Ben-Tal N. A putative molecular-activation switch in the transmembrane domain of erbB2. *Proc Natl Acad Sci U S A*. 2002;99(25):15937–15940.
11. Mineev KS, Bocharov EV, Pustovalova YE, Bocharova OV, Chupin VV, Arseniev AS. Spatial structure of the transmembrane domain heterodimer of ErbB1 and ErbB2 receptor tyrosine kinases. *J Mol Biol*. 2010;400(2):231–243.
12. Baselga J, Swain SM. Novel anticancer targets: revisiting ERBB2 and discovering ERBB3. *Nat Rev Cancer*. 2009;9(7):463–475.
13. Engelman JA. Targeting PI3K signalling in cancer: opportunities, challenges and limitations. *Nat Rev Cancer*. 2009;9(8):550–562.
14. Mountzios G, Planchard D, Besse B, et al. Mitogen-activated protein kinase activation in lung adenocarcinoma: a comparative study between ever smokers and never smokers. *Clin Cancer Res*. 2008;14(13):4096–4102.
15. Planchard D, Camara-Clayette V, Dorvault N, Soria JC, Fouret P. p38 Mitogen-activated protein kinase signaling, ERCC1 expression, and viability of lung cancer cells from never or light smoker patients. *Cancer*. 2012;118(20):5015–5025.

Funding

This study was supported by a Grant-in Aid for Scientific Research from the Ministry of Education, Culture, Sports, Science and Technology of Japan (25293302 to ST).

Note

H. Yamamoto, J. Soh, S. Miyoshi, and S. Toyooka conceived the project. K. Higasa, M. Sakaguchi, K. Shien, and K. Ichimura performed the experiments. H. Yamamoto, J. Soh, M. Furukawa, S. Hashida, N. Takigawa, K. Kiura, K. Tsukuda, and S. Toyooka collected the samples and assisted with the experiments. H. Yamamoto, K. Higasa, K. Shien, and K. Matsuo analyzed the data. H. Yamamoto, K. Higasa, M. Sakaguchi, F. Matsuda, and S. Toyooka prepared the manuscript with input from the other authors. S. Miyoshi, F. Matsuda, and S. Toyooka supervised the project. The authors declared no conflicts of interest.

Affiliations of authors: Department of Thoracic, Breast and Endocrinological Surgery (HY, KS, JS, MF, SH, KT, SM, ST), Department of Clinical Genomic Medicine (KS, ST), Department of Cell Biology (MS), Department of Pathology (KI), and Department of Hematology, Oncology and Respiratory Medicine (KK), Okayama University Graduate School of Medicine, Dentistry and Pharmaceutical Sciences, Okayama, Japan; Center for Genomic Medicine, Kyoto University School of Medicine, Kyoto, Japan (KH, FM); Department of General Internal Medicine 4, Kawasaki Medical School, Okayama, Japan (NT); Department of Preventive Medicine, Kyushu University Faculty of Medical Sciences, Fukuoka, Japan (KM).

Annals of human genetics

doi: 10.1111/ahg.12034

Quantitative Variation in Plasma Angiotensin-I Converting Enzyme Activity Shows Allelic Heterogeneity in the *ABO* Blood Group Locus

Chikashi Terao[1], Nervana Bayoumi[2], Colin A. McKenzie[3], Diana Zelenika[4,5], Shigeo Muro[6], Michiaki Mishima[6], The Nagahama Cohort Research Group[7], John M. C. Connell[8], Mark A. Vickers[9], G. Mark Lathrop[4,5,10], Martin Farrall[11,12], Fumihiko Matsuda[1] and Bernard D. Keavney[13,14]*

[1]*The Center for Genomic Medicine, Kyoto University Graduate School of Medicine, Kyoto, Japan*
[2]*Physiology Department, College of Medicine, King Saud University, Riyadh, Saudi Arabia*
[3]*Tropical Metabolism Research Unit, University of the West Indies, Mona, Jamaica*
[4]*Commisariat à l'énergie Atomique (CEA), Institut Genomique, Centre National de Genotypage, Evry, France*
[5]*Fondation Jean Dausset, Centre d'Etude du Polymorphisme Humain, Paris, France*
[6]*Department of Respiratory Medicine, Kyoto University Graduate School of Medicine, Kyoto, Japan*
[7]*The following investigators belonging to Kyoto University Graduate School of Medicine (Kyoto, Japan) were core members of the Nagahama Study Group: Takeo Nakayama (Department of Health Informatics); Shinji Kosugi (Department of Medical Ethics); Akihiro Sekine, Takahisa Kawaguchi, Ryo Yamada and Yasuharu Tabara (The Center for Genomic Medicine)*
[8]*College of Medicine, Dentistry and Nursing, University of Dundee, UK*
[9]*School of Medicine, University of Aberdeen, UK*
[10]*McGill University and Genome Quebec Innovation Center, Montreal, Canada*
[11]*Division of Cardiovascular Medicine, Radcliffe Department of Medicine, University of Oxford, Oxford, UK*
[12]*Wellcome Trust Centre for Human Genetics, University of Oxford, Oxford, UK*
[13]*Institute of Genetic Medicine, Newcastle University, UK*
[14]*Institute of Cardiovascular Sciences, Manchester University, UK*

Summary

Angiotensin-I converting enzyme (ACE) occupies a pivotal role in cardiovascular homeostasis. Major loci for plasma ACE have been identified at *ACE* on Chromosome 17 and at *ABO* on Chromosome 9. We sought to characterise the genetic architecture of plasma ACE at finer resolution in two populations. We carried out a GWAS in 1810 individuals of Japanese ethnicity; this identified signals at *ACE* and *ABO* that together accounted for nearly half of the population variability of the trait. We conducted measured haplotype analysis at the *ABO* locus in 1425 members of 248 British families using haplotypes of three SNPs, which together tagged the alleles responsible for the principal blood group antigens A1, A2, B and O. Type O alleles were associated with intermediate plasma ACE activity compared to Type A1 alleles (in whom plasma ACE activity was ~36% lower) and Type B alleles (in whom plasma ACE activity was ~36% higher). We demonstrated heterogeneity among A alleles: A2 alleles were associated with plasma ACE activity that was very similar to the O alleles. Variation at *ACE* accounted for 35% of the trait variance, and variation at *ABO* accounted for 15%. A further 10% could be ascribed to polygenic effects.

Keywords: ABO blood group, angiotensin-I converting enzyme, genome wide association study, QTL

Introduction

The renin–angiotensin system plays a critical role in cardiovascular homeostasis, regulating blood pressure, arterial tone and renal salt excretion. The angiotensin I-converting enzyme (ACE) converts circulating angiotensin-I, which is

*Corresponding author: Bernard D. Keavney, Institute of Genetic Medicine, Newcastle University, Central Parkway, NE1 3BZ, UK. Tel: +44 191 241 8615; Fax: +44 191 241 8666; E-mail: bernard.keavney@newcastle.ac.uk

biologically inactive, to the active angiotensin-II and degrades the vasodilator bradykinin. ACE occupies a pivotal position in the renin–angiotensin system: drugs which inhibit ACE, or which block the cellular receptor for the angiotensin-II generated by the action of ACE, are among the most widely prescribed agents in patients with coronary artery disease, hypertension and chronic renal disease (Yusuf et al., 2000). Plasma ACE activity is related to tissue ACE activity, and is strongly influenced by genetic factors, the largest such influence being due to polymorphic variation in the *ACE* (also known as *DCP1*) gene, which encodes ACE (Rigat et al., 1990; Keavney et al., 1998). Previous segregation and linkage analysis suggested the existence of a second major quantitative trait locus (QTL) influencing plasma ACE activity (McKenzie et al., 1995). A genome wide association study (GWAS) in a population of hypertensive patients of Han Chinese ancestry subsequently found this to be located at the *ABO* gene which encodes glycosyltransferases A and B (Chung et al., 2010). Global variation in the distribution of the alleles responsible for ABO blood groups is well described; we therefore sought to confirm the identity of the second principal locus influencing ACE activity and to estimate the proportions of phenotypic variance attributable to major gene effects in two additional populations from Japan and the United Kingdom.

Methods

Study Populations and ACE Phenotyping

The discovery cohort included 1830 volunteers recruited as a part of the Nagahama Prospective Genome Cohort for Comprehensive Human Bioscience (the Nagahama Study), a community-based prospective multiomics cohort study. The study has been described in detail elsewhere (Yoshimura et al., 2012); demographics of the cohort are summarised in Table S1. In brief, a total of 9809 volunteers from Nagahama City, Shiga Prefecture, Japan, were recruited for this study from 2008 to 2010. All participants completed a detailed health questionnaire. DNA, serum and plasma samples from all participants were obtained and stored for further analysis. Samples were kept on ice immediately after they were obtained from the participants and were promptly processed. Plasma was stored at –80°C. ACE activity was quantified by the method reported by Kasahara & Ashihara (1981). Patients receiving ACE inhibitor therapy were excluded from the analyses.

The replication cohort comprised 248 British families of Northern and Western European ancestry who participated in a quantitative genetic study of cardiovascular risk factors (Palomino-Doza et al., 2008). The population collection strategy has been previously described in detail (Gaukrodger et al., 2005). In brief, families were ascertained via a hypertensive proband between 1993 and 1996, and any sibship in the family (in the generation of the proband or his/her offspring) greater than three members quantitatively assessable for blood pressure was collected. Families were extended where additional hypertensives were encountered during collection; a total of 1425 individuals participated. Families underwent detailed cardiovascular phenotyping including a questionnaire, electrocardiographic and echocardiographic measurement and measurement of 24-hour ambulatory blood pressure using an automated monitor (Keavney et al., 2000; Mayosi et al., 2008). Demographics of the cohort are presented in Table S2. Blood was drawn into multiple anticoagulants, immediately put on ice and transported rapidly to a central facility for processing. ACE activity was assessed by HPLC using a synthetic substrate, as previously described (Chiknas, 1979).

Genotyping

The 1830 volunteers in the Japanese cohort were genotyped using the Infinium Human 610-Quad Bead Chip carrying 592,044 SNP markers on a Bead Station 500G Genotyping System (Illumina, Inc., San Diego, CA, USA). There were no subjects showing call rates lower than 0.99. Kinship analysis was performed using PLINK. Of the 20 pairs of samples showing high degrees of kinship (PI-HAT > 0.4), the sample with the lower call rate in each pair was removed. 165,591 SNPs were removed either due to call rate lower than 0.95, minor allele frequency of less than 0.05, or distorted Hardy-Weinberg equilibrium ($P < 10^{-7}$). Finally, the results of 426,453 SNP markers in 1810 subjects were used for the analysis.

Three SNPs at the ABO locus (rs505922, rs8176746 and rs8176750) were typed in the entire British family cohort using matrix-assisted laser desorption/ionisation—time of flight mass spectrometry (MALDI-TOF) on a Sequenom instrument (Sequenom, San Diego, CA, USA). ABO blood group in the British families was studied in a subset of 734 individuals by multiplex polymerase chain reaction (PCR). Two pairs of primers were used to amplify exons 6 and 7 of the *ABO* gene; the amplified fragments were digested with restriction endonucleases *Hpa*II and *Kpn*I and separated by gel electrophoresis. This enabled us to call genotypes at the SNPs rs8176719, rs1053878, rs8176743 and rs8176472. As previously reported, genotypes at these SNPs, considered together, identify the A1, A2, B, O1 and O2 blood group alleles (Seltsam et al., 2003).

Statistical Methods

A quantitative linear regression analysis was first performed in the Japanese cohort to find the polymorphisms associated with ACE activity. SNP genotype imputation for SNPs within and

flanking the *ACE* (20 SNPs) and *ABO* (43 SNPs) loci was performed in the Japanese samples using the MaCH (version 1.0.10) computer program with 500 Markov sampler rounds and 200 haplotype states (Li et al., 2010). A forward-selection stepwise regression analysis was performed to identify a parsimonious subset of associated SNPs from the *ACE* and *ABO* loci in the Japanese population. This analysis was based on imputed SNP dosages using linear regression models based on marginal sums of squares and the *stepwise* procedure in Stata™ v10.1 (Stata Corp, College Station, TX, USA) using a $P < 0.01$ criterion for adding SNPs to the model. Variance component proportions (R^2) were calculated from a supplementary analysis of variance based on sequential sums of squares.

Haplotyping of *ABO* in the British samples was performed using PHASE (version 2.1.1) specifying a parent-independent multiallelic model for both SNP and blood group variation. (Stephens et al., 2001; Stephens & Scheet, 2005) Pedigree analysis was performed using the Pedigree Analysis Package (PAP version 5.0) to fit maximum likelihood models including polygenic variance components (Hasstedt, 1993) to extended families; missing data is efficiently incorporated into this analysis (Elston & Stewart, 1971). For the measured haplotype analysis, the PAP quantitative major gene subroutine *qmlprmv* was modified to parametrise an additive (codominant) genetic model. Likelihoods were maximised with simultaneous estimation of haplotype frequencies assuming Hardy–Weinberg equilibrium, haplotype-specific effects on ACE activity, covariate effects, polygenic effects and residual individual-specific random (i.e. environmental) effects and estimates of standard errors were calculated with the bundled quasi-Newton nonlinear optimisation function GEMINI (Lalouel, 1979). Variance component proportions were calculated by hand using a standard additive genetic variance formula.

Table 1 Forward selection stepwise regression analysis of plasma ACE activity and GWAS SNPs in the Japanese cohort. R^2 shows the proportion of variance explained by each variable.

Locus	Variable	Beta	SE	*F*-statistic	*P*-value	R^2
	Age	0.0363	0.0040	84.32	1.13E-19	0.0229
ACE	rs4362	−3.0450	0.0849	1286.30	9.60E-213	0.3494
ABO	rs495828	1.4762	0.0982	225.75	3.81E-48	0.0613
ABO	rs8176746	1.5698	0.1154	184.97	3.66E-40	0.0502

Table 2 *ABO* haplotype analysis using PHASE 2.1.1 in British families. Common haplotypes assessed in the measured haplotype analysis are shown in bold.

rs505922	rs8176746	rs8176750	Blood group allele	Conditional probability	Frequency
C	**G**	**G**	**A1**	**0.9235**	**0.1719**
C	G	G	A2	0.0049	0.0009
C	G	G	B	0.0139	0.0026
C	G	G	O1	0.0271	0.0050
C	G	G	O2	0.0307	0.0057
C	G	del	A1	0.1541	0.0096
C	**G**	**del**	**A2**	**0.8333**	**0.0517**
C	G	del	O1	0.0011	0.0001
C	G	del	O2	0.0115	0.0007
C	**T**	**G**	**B**	**1.0000**	**0.0513**
C	T	del	A2	0.2244	0.0004
C	T	del	B	0.7756	0.0014
T	G	G	A1	0.0068	0.0047
T	G	G	B	0.0055	0.0038
T	**G**	**G**	**O1**	**0.9618**	**0.6709**
T	G	G	O2	0.0259	0.0180
T	G	del	A1	0.0377	0.0000
T	G	del	O1	0.9623	0.0002
T	T	G	O1	1.0000	0.0007

Results

GWAS for ACE Activity

The SNPs with the strongest association with ACE activity genome-wide are presented in Table S3. Two loci, *ACE* on Chromosome 17, and *ABO* on Chromosome 9, showed genome-wide significant association ($P < 5 \times 10^{-8}$) with plasma ACE activity (Fig. S1). SNPs mapping to the *ACE* (20 SNPs) and *ABO* (43 SNPs) loci and their immediate upstream and downstream flanking regions (50 kb, respectively) were selected for fine-mapping analysis and any missing genotype data was imputed. Stepwise linear regression then identified three SNPs with independent significant effects ($10^{-213} < P < 10^{-40}$): rs4362 at *ACE*; and rs495828 and rs8176746 at *ABO*, that together accounted for nearly half of the population variation in the trait (Table 1), with the *ACE* locus accounting for 35% and the *ABO* locus accounting for 11%.

Association between Haplotypes Defining Blood Groups and ACE Activity

Haplotypes of rs505922, rs8176746 and rs8176750 showed strong associations with alleles defining the different blood groups in the subset of the British families (734 samples) where blood groups were available (conditional tagging probabilities range from 0.83 to 1.00; Table 2). Haplotypes of these three SNPs that occurred at a frequency of >0.05 in the population, and accurately tagged alleles responsible for A1, A2, B and O1 phenotypes, were taken forward to the

Table 3 Measured haplotype analysis of plasma ACE activity in British families. The *ABO* haplotype is defined by rs505922, rs8176746 and rs8176750; the most strongly tagged blood group allele is shown in parentheses.

ABO haplotype (blood group allele)	Frequency	Mean	*SE*
TGG (O1)	0.647	9.295	0.084
CGG (A1)	0.212	5.989	0.231
CGdel (A2)	0.079	9.473	0.473
CTG (B)	0.063	12.808	0.528

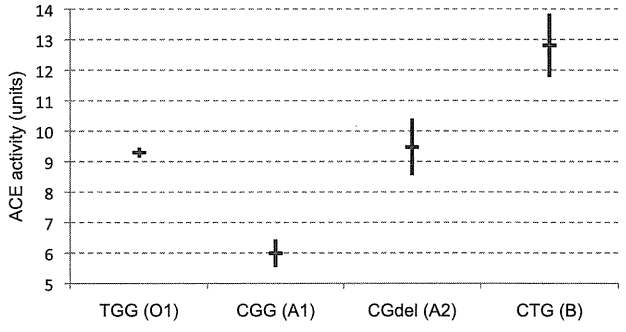

Figure 1 Measured haplotype analysis of plasma ACE activity in British families. The mean activities and 95% confidence intervals for each *ABO* haplotype are indicated by horizontal and vertical lines, respectively. *ABO* haplotypes are defined by rs505922, rs8176746 and rs8176750; the most strongly tagged blood group allele is shown in parentheses.

measured haplotype analysis of ACE activity in the total UK cohort. In the measured haplotype analyses, SNPs rs4295 and rs4392, previously shown in this cohort to tag the principal haplotype blocks influencing ACE activity at the *ACE* locus, were included as covariates. (Keavney et al., 1998) The measured haplotype analysis showed that the TGG haplotype of rs505922/rs8176746/rs8176750, which accurately tagged type O alleles and occurred at a frequency of ~65% in the population, was associated with an intermediate plasma ACE activity (Table 3). The CGG haplotype (frequency ~21%), which tagged type A1 alleles, was associated with a 36% lower plasma ACE activity than the TGG haplotype. The CTG haplotype (frequency ~6%), which tagged type B alleles, was associated with a 36% higher plasma ACE activity than the TGG haplotype. The CGdel haplotype (frequency ~8%), which tagged type A2 alleles, had a plasma ACE activity very similar to the TGG haplotype (Fig. 1). The measured haplotype analysis in the British families provided very similar estimates of variance components to the GWAS in the Japanese cohort: 35.4% of the variance was due to the *ACE* locus, and 13.0% to the *ABO* locus, with a further 9.6% attributable to polygenes and 42.1% to nongenetic residual variation.

Discussion

We have shown strong evidence for association between plasma ACE activity and genotypes at the *ABO* gene that define the major blood groups. Genome-wide analyses in a cohort of unrelated Japanese people confirmed that the strongest genetic influence on plasma ACE levels is located at the *ACE* gene itself on Chromosome 17 ($P = 1.55 \times 10^{-164}$ for rs4362) and demonstrated two further independent SNP effects at *ABO* (rs495828 and rs8176746). Stepwise regression suggested that the association at *ACE* accounted for 35% of the variability in the Japanese population and the two SNPs at *ABO* accounted for 11%. To confirm this finding, we typed SNPs at the *ABO* locus in a cohort of British families previously extensively genotypically characterised at the *ACE* locus. (McKenzie et al., 2001) Measured haplotype analysis in these families indicated that the haplotype characterizing group A1 was associated with the lowest plasma ACE level, the haplotypes characterizing groups O and A2 were associated with intermediate plasma ACE level, and the haplotype characterizing group B was associated with the highest plasma ACE level. The proportions of variance accounted for by the *ACE* and *ABO* loci in the British families were highly concordant with the Japanese cohort (35.4% and 13.0%, respectively) with an additional 9.6% attributable to polygenic effects. The *ACE* and *ABO* loci make the most substantial contribution to population variance in plasma ACE levels; also, there is appreciable heterogeneity in plasma ACE levels among the alleles specifying the two subgroups A1 and A2.

The *ABO* gene encodes a glycosyltransferase. Genetic variation in *ABO* results in the production of two differently named protein products: glycosyltransferase-A and glycosyltransferase-B. Glycosyltransferase-A transfers N-acetylgalactosamine to an acceptor glycoconjugate on the glycosphingolipid H-antigen, which is strongly present on the surface of red blood cells and more weakly present on a wide range of other cell types. Glycosyltransferase-B transfers D-galactose to the same position on the H-antigen. These glycosyltransferase activities define the blood group antigens A and B, respectively. AB heterozygotes have molecules with both A and B antigens present on the red cell surface. Mutations which inactivate the glycosyltransferase encoded by *ABO* result in nonmodification of the H-antigen, which characterises blood group O. A and B alleles are both dominant to O.

Previous studies have shown association between either *ABO* genotypes or ABO blood groups and plasma ACE activity. Cidl et al. found blood groups A and O to have similar levels of plasma ACE activity and groups AB and B to have progressively higher levels among 197 Caucasian subjects of Eastern European origin. (Cidl et al., 1996) Chung et al. performed a GWAS for plasma ACE activity among 1023 subjects with young-onset hypertension, replicating their findings in a